International Journal of Analysis and Applications

An Extension of the Gompertz Distribution for Modeling COVID-19 Mortality Dynamics

Ahmad Abubakar Suleiman[1,2,*], Hanita Daud[1], Aliyu Ismail Ishaq[3], Narinderjit Singh Sawaran Singh[4], Diaa S. Metwally[5], H. E. Semary[6] , Mohammed Elgarhy[7]

[1]Department of Fundamental and Applied Science, Universiti Teknologi PETRONAS, 32610, Seri Iskandar, Malaysia

[2]Department of Statistics, Aliko Dangote University of Science and Technology, Wudil 713281, Nigeria

[3]Department of Statistics, Ahmadu Bello University, Zaria, 810107, Nigeria

[4]Faculty of Data Science and Information Technology, INTI International University, Persiaran Perdana BBN Putra Nilai, Malaysia

[5]Department of Accounting, Faculty of Business, Imam Mohammad Ibn Saud Islamic University (IMSIU), Riyadh, 11432, Saudi Arabia

[6]Department of Mathematics and Statistics, Faculty of Science, Imam Mohammad Ibn Saud Islamic University (IMSIU), Riyadh 11432, Saudi Arabia

[7]Department of Basic Sciences, Higher Institute of Administrative Sciences, Belbeis, AlSharkia, Egypt

**Corresponding author:* ahmadabubakar31@gmail.com

ABSTRACT. The Gompertz distribution is widely used in medical and reliability studies, particularly for modeling mortality rates and failure data. However, it has limitations in capturing complex data behaviors, such as heavy tails and varying hazard rate shapes. This paper introduces the Odd Beta Prime-Gompertz (OBP-Gompertz) distribution, a four-parameter extension of the traditional Gompertz model. The OBP-Gompertz distribution offers flexibility in modeling various shapes of probability density functions, including right-skewed, left-skewed, heavy-tailed, light-tailed, and unimodal distributions. Its hazard function can accommodate multiple forms, such as increasing, decreasing, bathtub-shaped, and inverted bathtub-shaped curves, making it well-suited for mortality rate data. The paper investigates key statistical properties, including moments, moment generating function, quantile function, Rényi and Tsallis entropy measures. Parameters are estimated using maximum likelihood estimation, and the model's robustness is assessed through Monte Carlo simulations. The OBP-Gompertz model is applied to three real-world COVID-19 mortality datasets from China, the Netherlands, and Nepal. The results demonstrate that the OBP-Gompertz model provides superior fits compared to the traditional Gompertz and other models. This work highlights the OBP-Gompertz distribution as a valuable tool for survival analysis, reliability studies, and epidemiological research.

Received May 31, 2025

2020 Mathematics Subject Classification. 62E15.

Key words and phrases. Gompertz distribution; probability distribution; skewness; kurtosis; statistical modeling; infectious disease.

https://doi.org/10.28924/2291-8639-23-2025-206

ISSN: 2291-8639

1. Introduction

Statistical modeling of lifetime data plays an integral role across multiple disciplines, including engineering, biology, medicine, economics, and environmental sciences. The selection of an appropriate statistical distribution is critical to ensuring accurate and reliable modeling outcomes. Some widely used statistical distributions include the Gompertz, beta, logistic, Weibull, exponential, normal, and gamma models. Despite their usefulness, classical distributions often fall short in capturing real-world complexities such as extreme skewness, heavy tails, and high variability [1, 2]. These limitations necessitate the development of flexible models capable of addressing diverse data structures [3-5].

In biomedical research, skewness and kurtosis are common challenges arising from extreme values and outliers [6, 7]. Skewness refers to the asymmetry in data distributions, which may result in clustering on one side [8, 9]. For example, survival times of patients undergoing specific treatments often exhibit positive skewness due to the majority of patients having short survival times, while a few live significantly longer [10-13]. Negative skewness, on the other hand, may occur in physiological measurements like biomarker levels, where most values are high, but a few are unusually low due to specific health conditions [14-17]. Kurtosis, which measures the concentration of data in the tails, is another significant feature of biomedical datasets [18-21]. High kurtosis is often observed in clinical trials, reflecting the occurrence of rare, extreme reactions or outcomes [22, 23]. This behavior emphasizes the need for models that can effectively handle tail-heavy distributions to derive meaningful inferences about treatment efficacy and patient outcomes [24-28]. Additionally, biomedical data often exhibits considerable variability, driven by genetic diversity, environmental factors, lifestyle variations, and biological randomness [29-33]. This variability is further complicated by measurement errors and inconsistencies in data collection [34-36]. These challenges highlight the demand for advanced models capable of accurately describing such complex data structures [11, 37-40].

The Gompertz distribution is a well-established model for lifetime data and has been widely applied in various fields, particularly in demography, reliability analysis, and survival studies. First introduced by Gompertz [41], it is related to certain distributions within the Pearson family through a simple transformation. The Gompertz distribution has been extensively studied and applied in diverse fields. For instance, Johnson, et al. [42] utilized it for analyzing lifetime data, while Ohishi, et al. [43] explored its applications in computer science. Economos [44] applied the distribution in biological studies, and Bemmaor and Glady [45] used it in marketing science. Additional applications are discussed in studies by [46-50]. The cumulative distribution function (CDF) of the Gompertz distribution is given by:

$$M\left(x;\lambda,\eta\right)=1-e^{-\eta\left(e^{\lambda x}-1\right)},\quad x\geq 0,\lambda>0,\eta>0, \tag{1}$$

where $\lambda>0$ and $\eta>0$ are the scale and shape parameters, respectively.

The corresponding probability density function (PDF) is given by:

$$m(x;\lambda,\eta)=\lambda\eta e^{\lambda x}e^{-\eta\left(e^{\lambda x}-1\right)},\quad x\geq 0,\lambda>0,\eta>0. \tag{2}$$

Despite its usefulness, the Gompertz distribution has limitations in its flexibility to capture diverse data behaviors, especially for datasets exhibiting heavy tails. Moreover, the classical Gompertz model struggles to represent certain data patterns, such as bathtub-shaped and unimodal hazard rates, limiting its broader applicability, see, for example [51-55]. Bathtub-shaped hazard rates are characterized by high initial failure rates, followed by a period of stabilization and an eventual increase due to aging or wear-out effects [56]. Examples include human mortality rates and failure rates of certain mechanical systems. Similarly, unimodal hazard rates, where failure rates peak and then decline, are commonly observed in disease progression scenarios . For this reason, several generalizations of the Gompertz distribution have been developed by researchers to enhance its flexibility. Examples include the beta-Gompertz distribution [57], Gompertz-power series distributions [58], generalized Gompertz distribution [59], the three-parameter Gompertz distribution [60], unit-Gompertz distribution [61], Gompertz-Lindley distribution [62], and generalized gamma-Gompertz distribution [63].

The Odd Beta Prime Generalized (OBP-G) family of distributions, proposed by Suleiman, et al. [64], has facilitated the introduction of several generalized distributions. These include the OBP-Weibull distribution by [65] and the OBP-Gumbel distribution by [66]. Other extensions include the OBP-Kumaraswamy distribution by [67], the OBP-inverted Kumaraswamy by [68], the OBP-Burr X distribution by [69], the OBP-Fréchet distribution by [70], and OBP-exponential distribution by [71]. The CDF of the OBP-G family is defined as:

$$G(x;\alpha,\beta,\varsigma)=\frac{B_{\frac{M(x;\varsigma)}{1-M(x;\varsigma)}}(\alpha,\beta)}{B(\alpha,\beta)},\ \alpha,\beta>0,\ x,\varsigma\in\mathbb{R}^{+}, \tag{3}$$

where $M(x;\varsigma)$ is the baseline CDF, $B_{M(x;\varsigma)}(\alpha,\beta)$ is the incomplete beta function, $B(\alpha,\beta)$ is the beta function, α,β are shape parameters, and $\varsigma\in\mathbb{R}^{+}$ is the parameter of the parent model . The incomplete beta function $B_{M(x;\varsigma)}(\alpha,\beta)$ is given by:

$$B_{M(x;\varsigma)}(\alpha,\beta)=\int_{0}^{\frac{M(x;\varsigma)}{1-M(x;\varsigma)}}\frac{t^{\alpha-1}}{(1+t)^{\alpha+\beta}}dt,\quad \alpha,\beta>0,\ x\in\mathbb{R}^{+}.$$

The corresponding PDF of the OBP-G family is defined as:

$$g(x;\alpha,\beta,\varsigma)=\frac{\left(\frac{M(x;\varsigma)}{1-M(x;\varsigma)}\right)^{\alpha-1}}{B(\alpha,\beta)\left[1+\left(\frac{M(x;\varsigma)}{1-M(x;\varsigma)}\right)\right]^{\alpha+\beta}}\times\left(\frac{m(x;\varsigma)}{\left(1-M(x;\varsigma)\right)^{2}}\right),\ \alpha,\beta>0,\ x,\varsigma\in\mathbb{R}^{+}, \tag{4}$$

where $m(x;\varsigma)$ is the baseline PDF.

The first objective of this paper is to introduce a new four-parameter distribution referred to as the OBP-Gompertz distribution. This new distribution is developed by combining the OBP-G family and the traditional Gompertz model. The OBP-Gompertz distribution extends the Gompertz model, offering greater flexibility by accommodating heavy tails in the density function and exhibiting a versatile hazard function capable of taking forms such as bathtub-shaped, increasing, decreasing, and unimodal. This enhanced flexibility makes it particularly suitable for analyzing complex biomedical data, where such hazard rate patterns are often observed. The primary motivation for this study is to develop a flexible statistical model capable of effectively analyzing COVID-19 mortality data from countries such as China, the Netherlands, and Nepal. Mortality data often exhibit diverse patterns, including right-skewed, left-skewed, heavy, or light tails. The OBP-Gompertz distribution is designed to handle these complexities, making it a robust tool for modeling such data. Fig. 1 shows the study plan.

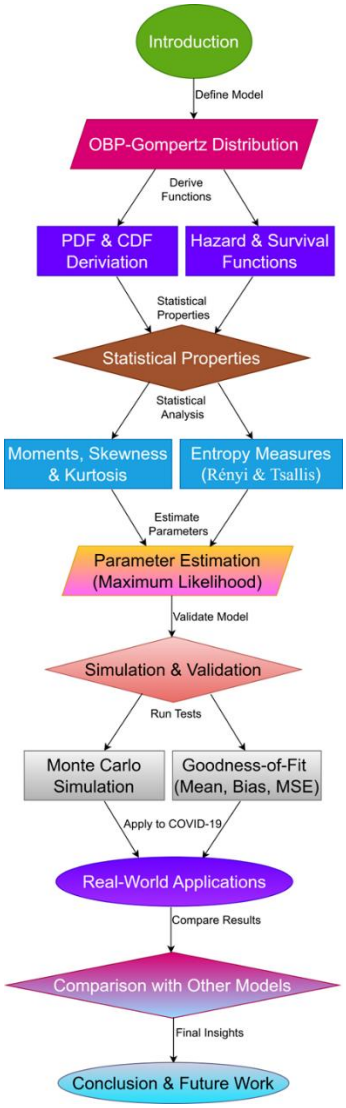

FIGURE 1. Study framework.

The fundamental objectives in establishing the OBP-Gompertz distribution are as follows:

1. To address variations in mortality data patterns, accommodate diverse characteristics such as right-skewed, left-skewed, heavy, or light tails, thereby enabling more accurate modeling of COVID-19 mortality data.
2. To capture diverse hazard rate shapes, including increasing, decreasing, bathtub, and upside-down bathtub patterns, which are vital for analyzing the complex dynamics of time-dependent mortality trends.
3. To enhance the fit for real-world datasets by generalizing the Gompertz distribution, allowing it to outperform many traditional statistical models when dealing with complex mortality data.
4. To support public health and epidemiology research by providing a robust statistical tool for studying regional and temporal variations in COVID-19 mortality, enabling better understanding and decision-making.
5. To investigate the statistical properties associated with the proposed model, including moments, linear representations, the quantile function, Rényi and Tsallis entropies, and the moment-generating function.
6. To assess the performance of the OBP-Gompertz model parameters through maximum likelihood estimation and validation via Monte Carlo simulations.
7. To demonstrate the application of the OBP-Gompertz distribution by analyzing COVID-19 mortality data from China, the Netherlands, and Nepal, showcasing its ability to provide meaningful insights and enable effective cross-country comparisons.

This paper is organized into seven sections. Section II introduces the OBP-Gompertz model and its distributional properties, including the hazard and survival functions. Section III delves into the structural characteristics of the model. Section IV outlines the methods for parameter estimation. Section V presents simulation studies to evaluate the robustness and efficiency of the model parameters. Section VI demonstrates the practical applicability of the OBP-Gompertz model by applying it to COVID-19 mortality data from China, the Netherlands, and Nepal. Finally, Section VII concludes the paper with a summary of key findings and recommendations for future research.

2. The OBP-Gompertz Distribution

This section derives the OBP-Gompertz distribution by utilizing the OBP-G family. The expressions for the CDF, PDF, validity checks, survival function, and hazard function of the OBP-Gompertz distribution are presented. Additionally, numerical and graphical representations of the CDF, PDF, survival function, and hazard function are provided, highlighting their unique and distinct shapes.

The CDF of the OBP-Gompertz distribution is expressed in the following equation. This representation is obtained by substituting the CDF specified in (1) with the CDF from (3):

$$F(x;\alpha,\beta,\lambda,\eta)=\frac{B_{1-e^{-\eta\left(e^{\lambda x}-1\right)}}(\alpha,\beta)}{B(\alpha,\beta)},\quad x>0,\alpha,\beta,\lambda,\eta>0. \tag{5}$$

The PDF of the OBP-Gompertz distribution, substituting (1) and (2) into the general OBP-G PDF in (4):

$$f(x;\alpha,\beta,\lambda,\eta)=\frac{\lambda\eta e^{\lambda x}e^{-\eta\left(e^{\lambda x}-1\right)}.\left[1-e^{-\eta\left(e^{\lambda x}-1\right)}\right]^{\alpha-1}.\left[e^{-\eta\left(e^{\lambda x}-1\right)}\right]^{\beta-1}}{B(\alpha,\beta)},\quad x>0,\alpha,\beta,\lambda,\eta>0. \tag{6}$$

Figs. 2 and 3 illustrate the flexibility of the OBP-Gompertz distribution in modeling diverse data patterns. The CDFs in Fig. 2 highlight its ability to adapt to varying growth trends, from steep initial increases that plateau to more gradual, steady growth, reflecting the diverse progression of COVID-19 mortality rates across populations. Fig. 3, presenting the PDFs, further emphasizes this versatility, presenting shapes that are right-skewed, left-skewed, heavy-tailed, light-tailed, and moderately skewed. This adaptability is particularly relevant for modeling phenomena like COVID-19 mortality, where most cases are mild, but a smaller fraction exhibits severe or fatal outcomes. The presence of heavy tails also enables the model to account for rare but extreme events, such as unexpected spikes in mortality rates. Overall, the OBP-Gompertz distribution's ability to capture both common trends and outliers makes it a robust and promising tool for analyzing complex biomedical data.

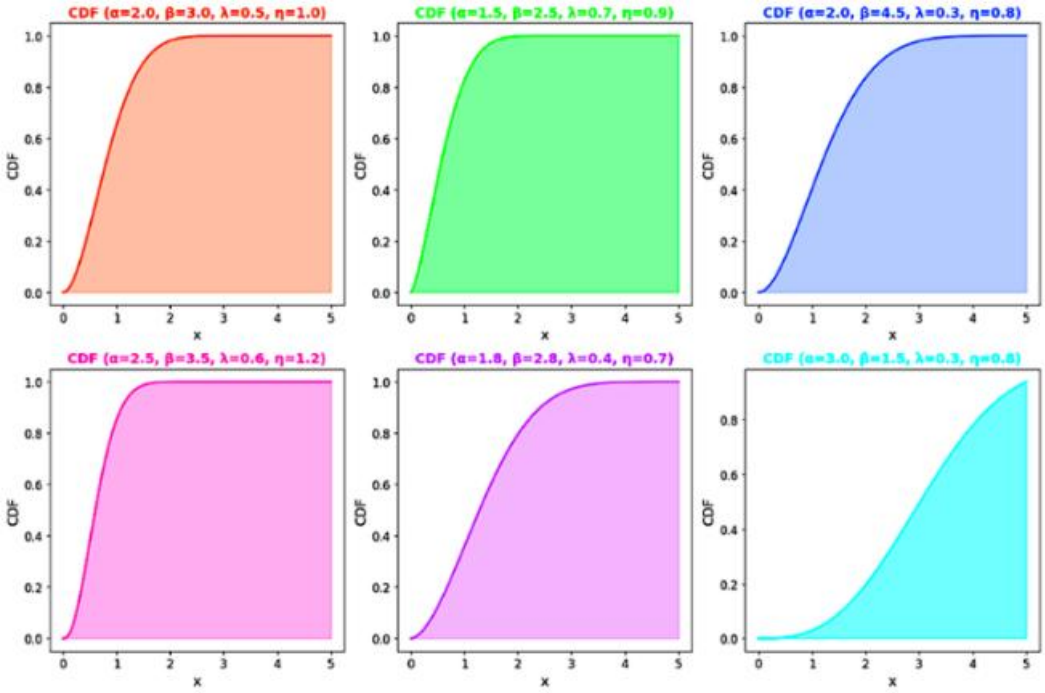

FIGURE 2. Possible shapes of the OBP-Gompertz CDF for various parameter combinations.

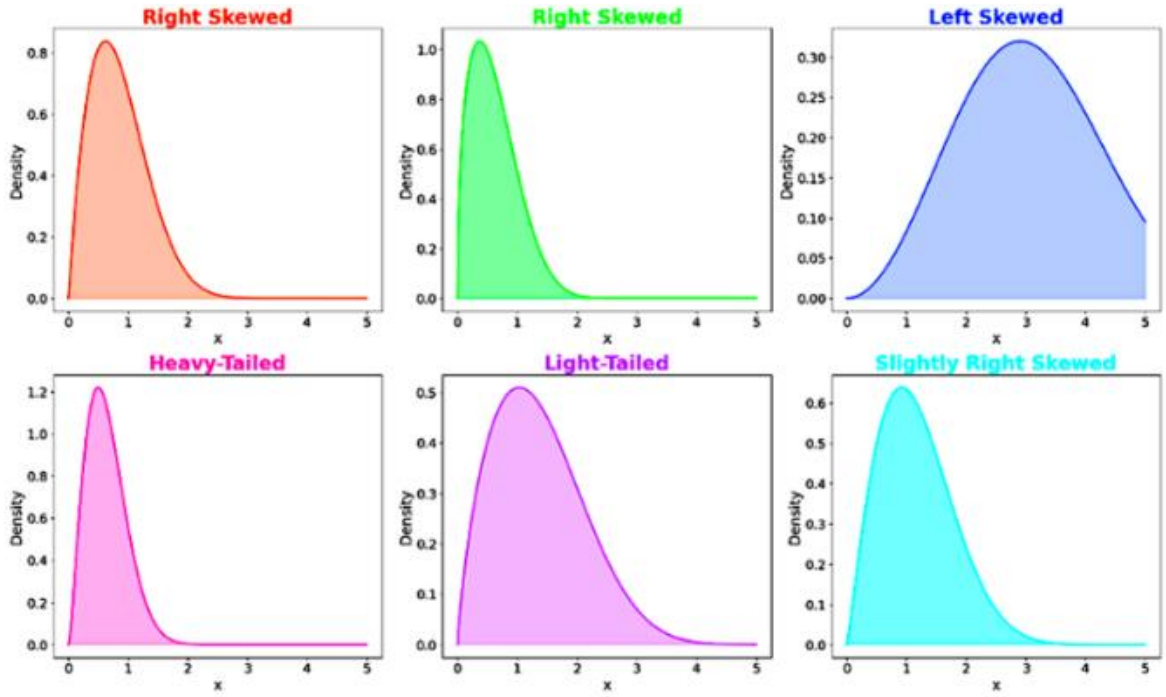

FIGURE 3. Possible shapes of the OBP-Gompertz PDF for various parameter combinations.

In Table 1, the numerical results of the CDF and PDF of the OBP-Gompertz distribution are presented for various combinations of the parameters $\eta = 0.5, \eta = 0.7,$ and $\eta = 1.2$, with varying $\alpha, \beta,$ and λ. This table illustrates how the CDF and PDF evolve with different parameter values, shedding light on the distribution's capacity to model diverse datasets. The analysis covers different values of $\alpha, \beta,$ and λ, providing insights into how the probability of an event occurring and the rate of that occurrence change under varying conditions. At smaller values of x, the CDF is closer to 1, meaning the event is more likely to have occurred, while the PDF shows the density of this likelihood. For example, with $\alpha = 1, \beta = 2, \lambda = 0.5$, the CDF is higher, indicating a greater likelihood of event occurrence at the initial stages. As x increases, the CDF decreases, and the PDF starts to show the rate at which this probability changes. The transition in these values across different η settings emphasize how the OBP-Gompertz distribution can capture shifts in event likelihood and rate over time.

The parameter η plays a pivotal role in shaping the distribution's behavior. As η increases, the shape of the CDF becomes steeper, and the PDF tends to concentrate more around certain values. For instance, when $\eta = 1.2$, the CDF decreases more rapidly, reflecting a higher rate of change in the probability of the event. Conversely, for $\eta = 0.5$, the CDF decays more gradually, and the PDF exhibits a more spread-out distribution. This highlights how η governs the distribution's sensitivity to changes in x and influences the event's likelihood over time.

Additionally, the values of α, β, and λ show how the distribution adapts to different risk and survival scenarios. Increasing β leads to higher CDF values and lower PDF values at smaller x, indicating a slower rate of event occurrence. Similarly, increasing λ results in a more pronounced change in the PDF, reflecting a faster rate of

Change in the probability density. These behaviors demonstrate the flexibility of the OBP-Gompertz distribution in modeling different risk profiles and survival patterns. Overall, the OBP-Gompertz distribution proves to be a powerful tool for capturing a wide range of survival and risk dynamics. Its ability to adjust the tail behavior and rate of occurrence through parameter variation makes it particularly valuable in fields where precise modeling of these factors is essential. The results in Table 1 demonstrate the distribution's versatility in handling diverse conditions and offer valuable insights into how the likelihood of events and their rates evolve across different parameter settings.

Fig. 4 presents the 3D PDF and contour plots of the OBP-Gompertz distribution for selected parameter combinations. The 3D plots visualize the overall shape of the PDF, while the contour plots provide a detailed view of the density landscape. These visualizations provide insights into the distribution's shape and behavior under different conditions. For example, the plot $(\alpha = 1.5, \beta = 1.5)$ shows a relatively symmetric PDF, with the peak occurring around $\lambda = 2.5$ and $\eta = 2.5$. The contour lines indicate that the density decreases as we move away from the peak in any direction. The plot $(\alpha = 2.0, \beta = 1.0)$ shows a slightly right-skewed PDF, with the peak occurring around $\lambda = 2$ and $\eta = 2$. The contour lines indicate that the density decreases as we move away from the peak, with a steeper decline in the right tail. The plot $(\alpha = 3.0, \beta = 0.5)$ shows a more pronounced right-skewed PDF, with the peak occurring around $\lambda = 2$ and $\eta = 2.5$. The contour lines indicate a rapid decrease in density as we move to the right of the peak, highlighting the distribution's heavy tail. By examining these plots, we can observe the flexibility of the OBP-Gompertz distribution in capturing a wide range of shapes, from symmetric to highly skewed. This flexibility makes the OBP-Gompertz distribution a powerful tool for modeling various real-world phenomena.

A. Validation of the OBP-Gompertz Distribution

To confirm that $f(x;\alpha,\beta,\lambda,\eta)$ is a valid PDF, we must show that:

$$\int_0^\infty f(x;\alpha,\beta,\lambda,\eta)\,dx = 1. \tag{7}$$

To verify this, we substitute (6) into (7):

$$\int_0^\infty f(x;\alpha,\beta,\lambda,\eta)dx = \frac{1}{B(\alpha,\beta)}\int_0^\infty \lambda\eta e^{\lambda x} e^{-\eta\left(e^{\lambda x}-1\right)}.\left(1-e^{-\eta\left(e^{\lambda x}-1\right)}\right)^{\alpha-1}.\left(e^{-\eta\left(e^{\lambda x}-1\right)}\right)^{\beta-1} dx. \tag{8}$$

Let:

$$u = 1 - e^{-\eta\left(e^{\lambda x}-1\right)}, \Rightarrow du = \lambda\eta e^{\lambda x} e^{-\eta\left(e^{\lambda x}-1\right)} dx. \tag{9}$$

Thus, the integral in (8) becomes:

$$\int_0^{\infty} f\left(x;\alpha,\beta,\lambda,\eta\right)dx = \frac{1}{B(\alpha,\beta)} \int_0^1 u^{\alpha-1}\left(1-u\right)^{\beta-1} du. \tag{10}$$

The integral $\int_0^1 u^{\alpha-1}\left(1-u\right)^{\beta-1} du$ is the definition of the Beta function, $B(\alpha,\beta)$:

$$\int_0^1 u^{\alpha-1}\left(1-u\right)^{\beta-1} du = B(\alpha,\beta). \tag{11}$$

Thus, (10) simplifies to:

$$\int_0^{\infty} f\left(x;\alpha,\beta,\lambda,\eta\right)dx = \frac{1}{B(\alpha,\beta)}.B(\alpha,\beta) = 1. \tag{12}$$

This confirms that $f\left(x;\alpha,\beta,\lambda,\eta\right)$ is a valid PDF.

B. Survival Function of OBP-Gompertz Distribution

The survival function $S(x)$ of the OBP-Gompertz distribution is expressed as:

$$S\left(x;\alpha,\beta,\lambda,\eta\right) = 1 - \left(\frac{B_{1-e^{-\eta\left(e^{\lambda x}-1\right)}}(\alpha,\beta)}{B(\alpha,\beta)} \right), \quad x>0, \alpha,\beta,\lambda,\eta>0. \tag{13}$$

C. Hazard Function of OBP-Gompertz Distribution

The hazard function $h(x)$ of the OBP-Gompertz distribution is expressed as:

$$h\left(x;\alpha,\beta,\lambda,\eta\right) = \frac{\lambda\eta e^{\lambda x} e^{-\eta\left(e^{\lambda x}-1\right)} .\left(1-e^{-\eta\left(e^{\lambda x}-1\right)}\right)^{\alpha-1} .\left(e^{-\eta\left(e^{\lambda x}-1\right)}\right)^{\beta-1}}{B(\alpha,\beta)\left\{1-\left(\frac{B_{1-e^{-\eta\left(e^{\lambda x}-1\right)}}(\alpha,\beta)}{B(\alpha,\beta)} \right)\right\}}. \tag{14}$$

Figs. 5 and 6 highlight the flexibility of the OBP-Gompertz distribution in capturing a variety of survival and hazard function patterns, making it highly suitable for modeling COVID-19 mortality dynamics. Fig. 5 reveals the broad range of survival function shapes, from steep initial drops to gradual declines, which align with different survival probabilities based on parameter combinations. This flexibility is especially useful in biomedical research, where survival functions often represent patient outcomes under varying disease progressions and treatment effects. Similarly, Fig. 6 demonstrates the ability of the OBP-Gompertz distribution to model diverse hazard rate patterns, including decreasing, increasing, bathtub-shaped, and upside-down bathtub-shaped patterns. These hazard functions align with the varying mortality

risks observed during the pandemic, capturing dynamics such as sudden surges, steady declines, or prolonged risk periods. Together, these figures demonstrate the OBP-Gompertz distribution's potential as a robust tool for analyzing and understanding the complex mortality patterns associated with COVID-19.

In Table 2, the survival and hazard functions of the OBP-Gompertz distribution are presented for various combinations of the parameters $\alpha, \beta, \lambda,$ and η. The table demonstrates how these functions vary with different parameter values, offering insights into the flexibility and versatility of the OBP-Gompertz distribution in modeling diverse datasets. The analysis spans different values of $\eta = 0.5, \eta = 0.7, \eta = 1.2$ and highlights how the survival probabilities and hazard rates evolve with changes in the $\alpha, \beta,$ and λ parameters, as well as the variable x.

At smaller values of x, the survival probabilities are higher, meaning the event is less likely to occur. For example, at $x = 0.1, \eta = 0.5, \alpha = 1, \beta = 2,$ and $\lambda = 0.5$, the survival probability is 0.853753, and the hazard rate is 0.790569. As x increases, survival probabilities drop, and hazard rates rise. This shows the risk of the event grows over time. The pattern holds across different parameter combinations, highlighting the distribution's ability to handle various survival and risk scenarios. The parameter η significantly impacts the survival and hazard trends. Higher η values, such as $\eta = 1.2$, lead to higher survival probabilities and lower hazard rates at small x values. However, these trends reverse sharply as x grows. For instance, at $x = 5$ with $\alpha = 1, \beta = 2,$ and $\lambda = 0.5$, the survival probability is 0.326922 when $\eta = 0.5$, compared to 0.031767 when $\eta = 1.2$. Similarly, the hazard rate increases from 0.111803 for $\eta = 0.5$ to 0.827838 for $\eta = 1.2$. This illustrates how η shapes the tail behavior and risk dynamics.

The distribution also adapts well to different parameter settings, offering versatility in modeling risks. For example, increasing β from 2 to 2.5 raises survival probabilities and lowers hazard rates for similar x values. This shows the scale parameter's role in moderating how fast survival decreases and risk grows. Likewise, increasing α to 1.5 results in higher survival rates at smaller x and slower hazard growth, reflecting the shape parameter's effect on the distribution's steepness. Overall, the OBP-Gompertz distribution effectively captures various survival and hazard patterns. Its flexibility makes it ideal for real-world applications, especially those needing precise control over risks and tail behaviors. These results demonstrate the distribution's ability to provide meaningful insights into survival and risk dynamics under diverse conditions.

The 3D and contour plots in Fig. 7 provide a comprehensive view of the hazard function of the OBP-Gompertz distribution under specific parameter constraints such as $\alpha = 2.5, \beta = 2.0$; $\alpha = 1.0, \beta = 2.5$; $\alpha = 3.0, \beta = 0.5$. The 3D plot visualizes the overall shape of the

hazard function as a function of λ and η, while the contour plot highlights specific regions of interest and the rate of change. The contour lines reveal how the hazard rate changes with respect to λ and η. As λ increases, the hazard rate generally increases, indicating a higher risk of failure. However, the impact of η on the hazard rate is more complex, demonstrating the distribution's flexibility in capturing various hazard rate patterns.

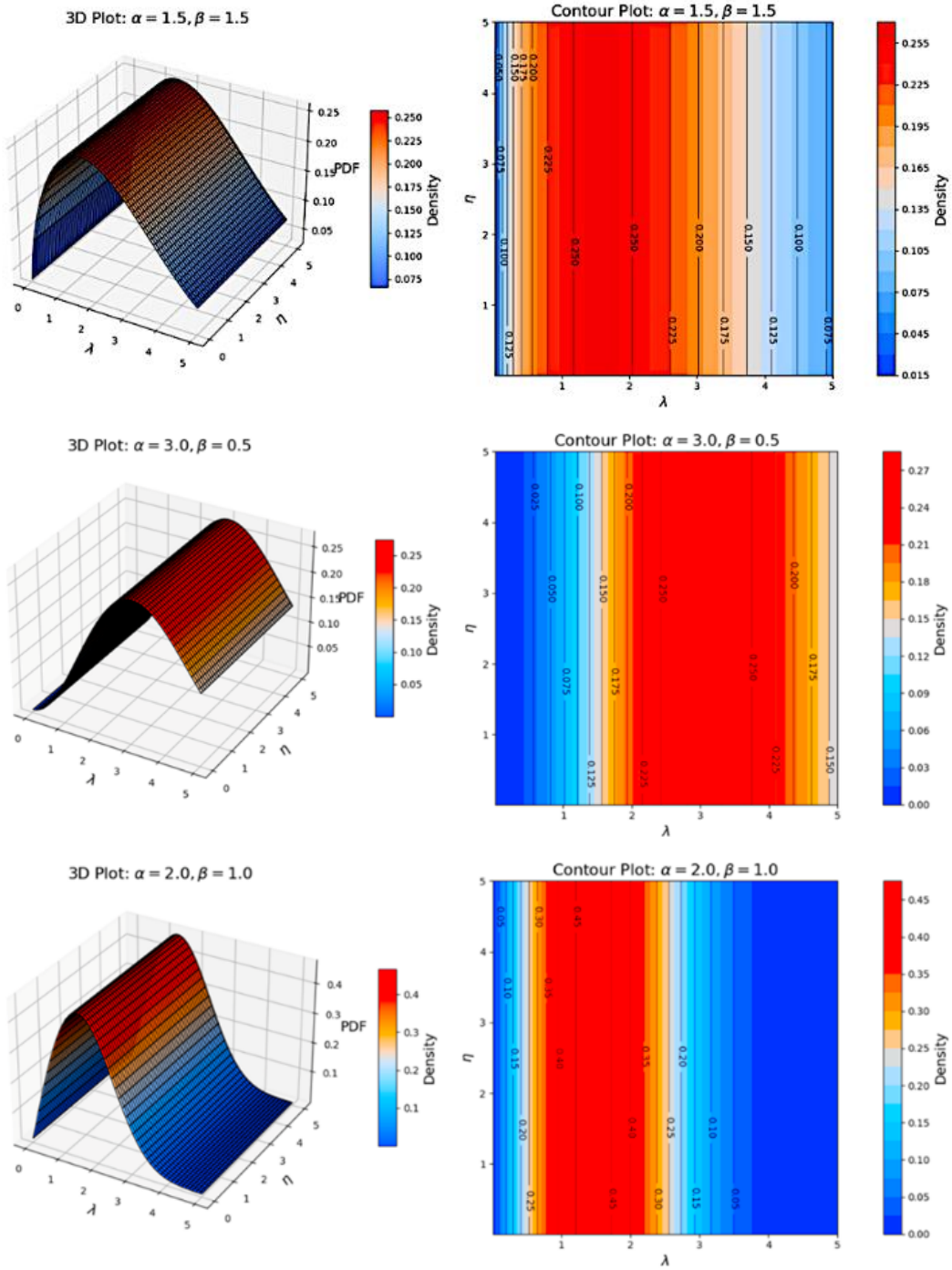

FIGURE 4. 3D PDF and contour plots of the OBP-Gompertz distribution.

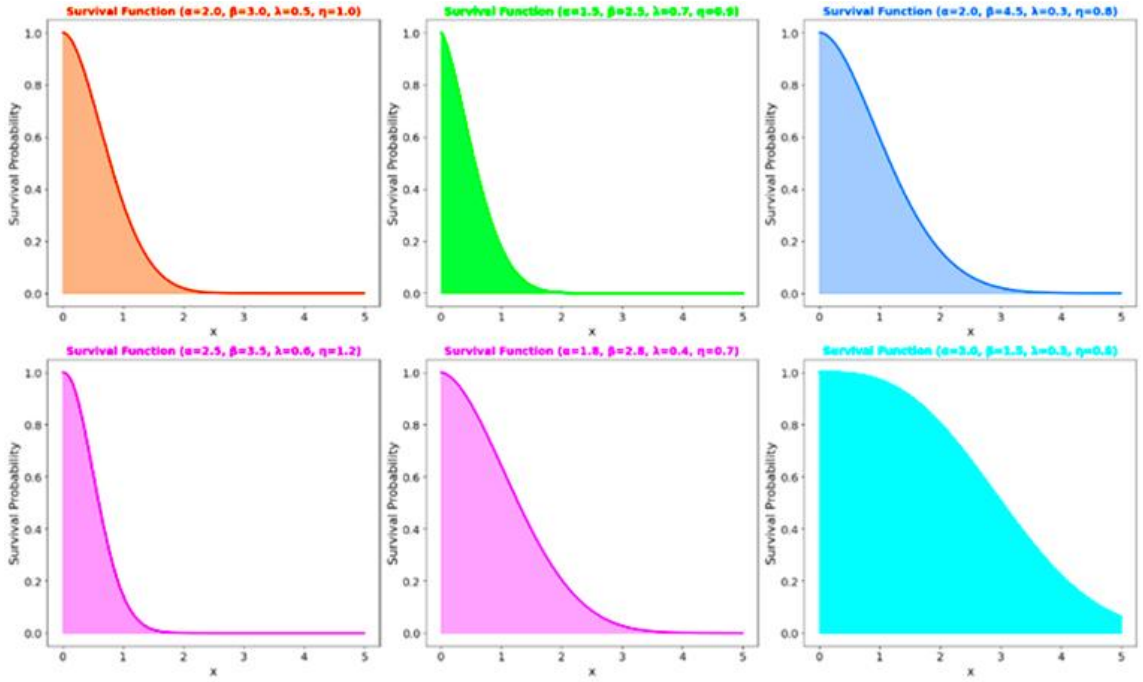

FIGURE 5. Possible shapes of the OBP-Gompertz survival function.

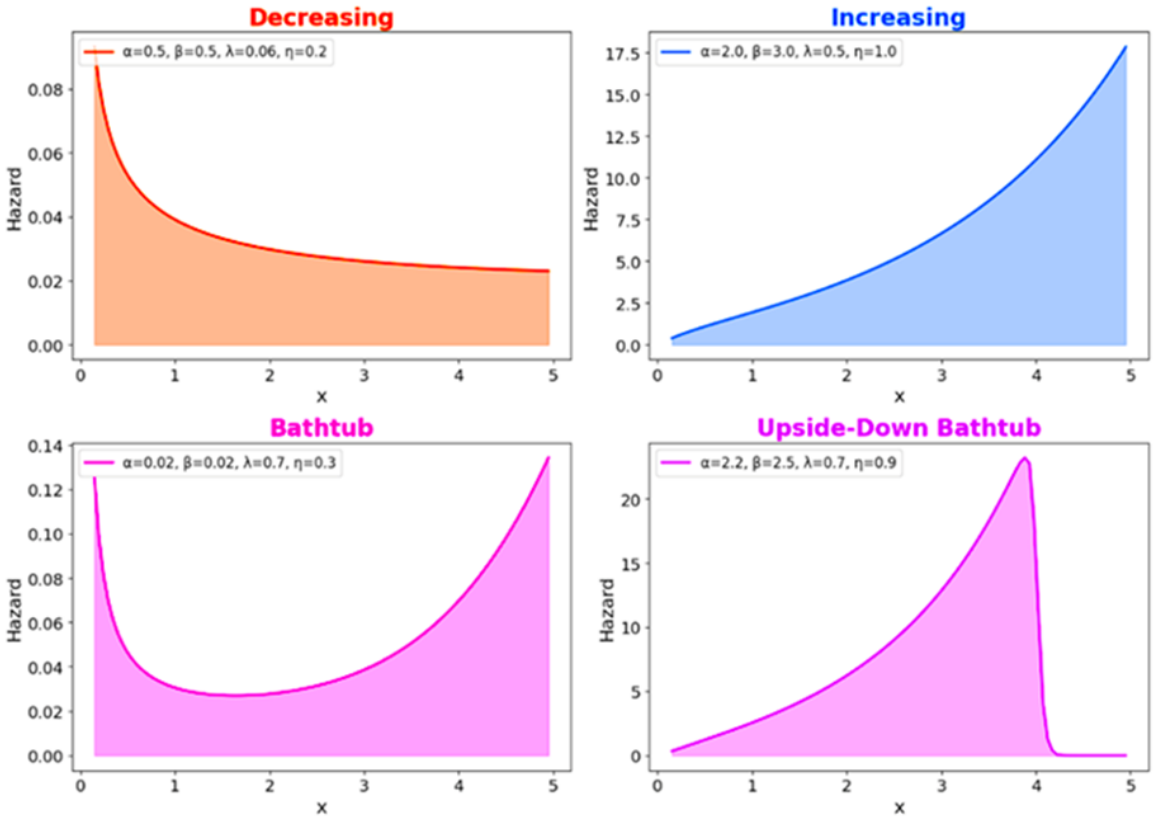

FIGURE 6. Possible shapes of the OBP-Gompertz hazard function.

TABLE 1. Numerical results for the CDF and PDF of the OBP-Gompertz distribution

				$\eta = 0.5$		$\eta = 0.7$		$\eta = 1.2$	
x	α	β	λ	CDF	PDF	CDF	PDF	CDF	PDF
0.100000	1	2	0.5	0.146247	0.674951	0.094948	0.632036	0.094948	0.632036
0.644444	1	2	0.5	0.330609	0.208462	0.30762	0.276476	0.30762	0.276476
1.188889	1	2	0.5	0.420263	0.132923	0.431285	0.188982	0.431285	0.188982
1.733333	1	2	0.5	0.482259	0.098313	0.520413	0.142321	0.520413	0.142321
2.277778	1	2	0.5	0.529809	0.077886	0.589208	0.112315	0.589208	0.112315
2.822222	1	2	0.5	0.568278	0.064246	0.644302	0.091195	0.644302	0.091195
3.366667	1	2	0.5	0.600453	0.054439	0.689486	0.075507	0.689486	0.075507
3.911111	1	2	0.5	0.627987	0.047027	0.727172	0.063426	0.727172	0.063426
4.455556	1	2	0.5	0.65195	0.041222	0.759007	0.053877	0.759007	0.053877
5.000000	1	2	0.5	0.673078	0.036551	0.786172	0.046179	0.786172	0.046179
0.100000	1	2.5	0.5	0.146247	0.674951	0.094948	0.632036	0.094948	0.632036
0.644444	1	2.5	0.5	0.330609	0.208462	0.30762	0.276476	0.30762	0.276476
1.188889	1	2.5	0.5	0.420263	0.132923	0.431285	0.188982	0.431285	0.188982
1.733333	1	2.5	0.5	0.482259	0.098313	0.520413	0.142321	0.520413	0.142321
2.277778	1	2.5	0.5	0.529809	0.077886	0.589208	0.112315	0.589208	0.112315
2.822222	1	2.5	0.5	0.568278	0.064246	0.644302	0.091195	0.644302	0.091195
3.366667	1	2.5	0.5	0.600453	0.054439	0.689486	0.075507	0.689486	0.075507
3.911111	1	2.5	0.5	0.627987	0.047027	0.727172	0.063426	0.727172	0.063426
4.455556	1	2.5	0.5	0.65195	0.041222	0.759007	0.053877	0.759007	0.053877
5.000000	1	2.5	0.5	0.673078	0.036551	0.786172	0.046179	0.786172	0.046179
0.100000	1	3	0.5	0.146247	0.674951	0.094948	0.632036	0.094948	0.632036
0.644444	1	3	0.5	0.330609	0.208462	0.30762	0.276476	0.30762	0.276476
1.188889	1	3	0.5	0.420263	0.132923	0.431285	0.188982	0.431285	0.188982
1.733333	1	3	0.5	0.482259	0.098313	0.520413	0.142321	0.520413	0.142321
2.277778	1	3	0.5	0.529809	0.077886	0.589208	0.112315	0.589208	0.112315
2.822222	1	3	0.5	0.568278	0.064246	0.644302	0.091195	0.644302	0.091195
3.366667	1	3	0.5	0.600453	0.054439	0.689486	0.075507	0.689486	0.075507
3.911111	1	3	0.5	0.627987	0.047027	0.727172	0.063426	0.727172	0.063426
4.455556	1	3	0.5	0.65195	0.041222	0.759007	0.053877	0.759007	0.053877
5.000000	1	3	0.5	0.673078	0.036551	0.786172	0.046179	0.786172	0.046179
0.100000	1.5	2	0.5	0.085076	0.610122	0.043584	0.447513	0.043584	0.447513
0.644444	1.5	2	0.5	0.302067	0.292111	0.270372	0.374731	0.270372	0.374731
1.188889	1.5	2	0.5	0.434067	0.203241	0.450974	0.290743	0.450974	0.290743
1.733333	1.5	2	0.5	0.53014	0.15356	0.589686	0.221421	0.589686	0.221421
2.277778	1.5	2	0.5	0.604281	0.120793	0.694786	0.16697	0.694786	0.16697
2.822222	1.5	2	0.5	0.663351	0.097401	0.77378	0.125089	0.77378	0.125089
3.366667	1.5	2	0.5	0.711399	0.079897	0.832818	0.093263	0.832818	0.093263
3.911111	1.5	2	0.5	0.751068	0.06638	0.876752	0.069271	0.876752	0.069271
4.455556	1.5	2	0.5	0.784192	0.055702	0.909335	0.051291	0.909335	0.051291
5.000000	1.5	2	0.5	0.812101	0.047121	0.93343	0.037878	0.93343	0.037878
0.100000	1.5	2.5	0.5	0.085076	0.610122	0.043584	0.447513	0.043584	0.447513

TABLE 2. Numerical results for the survival and hazard functions of the proposed model

				$\eta = 0.5$		$\eta = 0.7$		$\eta = 1.2$	
x	α	β	λ	Survival	Hazard	Survival	Hazard	Survival	Hazard
0.100000	1	2	0.5	0.853753	0.790569	0.905052	0.698342	0.968945	0.378574
0.644444	1	2	0.5	0.669391	0.311421	0.692380	0.399312	0.744445	0.549526
1.188889	1	2	0.5	0.579737	0.229282	0.568715	0.332296	0.540438	0.621126
1.733333	1	2	0.5	0.517741	0.189889	0.479587	0.296759	0.380051	0.669773
2.277778	1	2	0.5	0.470191	0.165647	0.410792	0.273410	0.261136	0.707381
2.822222	1	2	0.5	0.431722	0.148814	0.355698	0.256384	0.176133	0.738362
3.366667	1	2	0.5	0.399547	0.136251	0.310514	0.243169	0.116962	0.764876
3.911111	1	2	0.5	0.372013	0.126412	0.272828	0.232476	0.076627	0.788154
4.455556	1	2	0.5	0.348050	0.118437	0.240993	0.223562	0.049605	0.808969
5.000000	1	2	0.5	0.326922	0.111803	0.213828	0.215962	0.031767	0.827838
0.100000	1	2.5	0.5	0.853753	0.790569	0.905052	0.698342	0.968945	0.378574
0.644444	1	2.5	0.5	0.669391	0.311421	0.692380	0.399312	0.744445	0.549526
1.188889	1	2.5	0.5	0.579737	0.229282	0.568715	0.332296	0.540438	0.621126
1.733333	1	2.5	0.5	0.517741	0.189889	0.479587	0.296759	0.380051	0.669773
2.277778	1	2.5	0.5	0.470191	0.165647	0.410792	0.273410	0.261136	0.707381
2.822222	1	2.5	0.5	0.431722	0.148814	0.355698	0.256384	0.176133	0.738362
3.366667	1	2.5	0.5	0.399547	0.136251	0.310514	0.243169	0.116962	0.764876
3.911111	1	2.5	0.5	0.372013	0.126412	0.272828	0.232476	0.076627	0.788154
4.455556	1	2.5	0.5	0.348050	0.118437	0.240993	0.223562	0.049605	0.808969
5.000000	1	2.5	0.5	0.326922	0.111803	0.213828	0.215962	0.031767	0.827838
0.100000	1	3	0.5	0.853753	0.790569	0.905052	0.698342	0.968945	0.378574
0.644444	1	3	0.5	0.669391	0.311421	0.692380	0.399312	0.744445	0.549526
1.188889	1	3	0.5	0.579737	0.229282	0.568715	0.332296	0.540438	0.621126
1.733333	1	3	0.5	0.517741	0.189889	0.479587	0.296759	0.380051	0.669773
2.277778	1	3	0.5	0.470191	0.165647	0.410792	0.273410	0.261136	0.707381
2.822222	1	3	0.5	0.431722	0.148814	0.355698	0.256384	0.176133	0.738362
3.366667	1	3	0.5	0.399547	0.136251	0.310514	0.243169	0.116962	0.764876
3.911111	1	3	0.5	0.372013	0.126412	0.272828	0.232476	0.076627	0.788154
4.455556	1	3	0.5	0.348050	0.118437	0.240993	0.223562	0.049605	0.808969
5.000000	1	3	0.5	0.326922	0.111803	0.213828	0.215962	0.031767	0.827838
0.100000	1.5	2	0.5	0.914924	0.666855	0.956416	0.467907	0.992107	0.142640
0.644444	1.5	2	0.5	0.697933	0.418538	0.729628	0.513592	0.797138	0.633273
1.188889	1.5	2	0.5	0.565933	0.359125	0.549026	0.529561	0.505255	1.033607
1.733333	1.5	2	0.5	0.469860	0.326822	0.410314	0.539639	0.260350	1.397488
2.277778	1.5	2	0.5	0.395719	0.305248	0.305214	0.547060	0.110765	1.738808
2.822222	1.5	2	0.5	0.336649	0.289323	0.226220	0.552954	0.039313	2.064027
3.366667	1.5	2	0.5	0.288601	0.276842	0.167182	0.557852	0.011730	2.376855
3.911111	1.5	2	0.5	0.248932	0.266659	0.123248	0.562049	0.002960	2.679678
4.455556	1.5	2	0.5	0.215808	0.258111	0.090665	0.565724	0.000635	2.974158
5.000000	1.5	2	0.5	0.187899	0.250778	0.066570	0.568994	0.000116	3.261508
0.100000	1.5	2.5	0.5	0.914924	0.666855	0.956416	0.467907	0.992107	0.142640

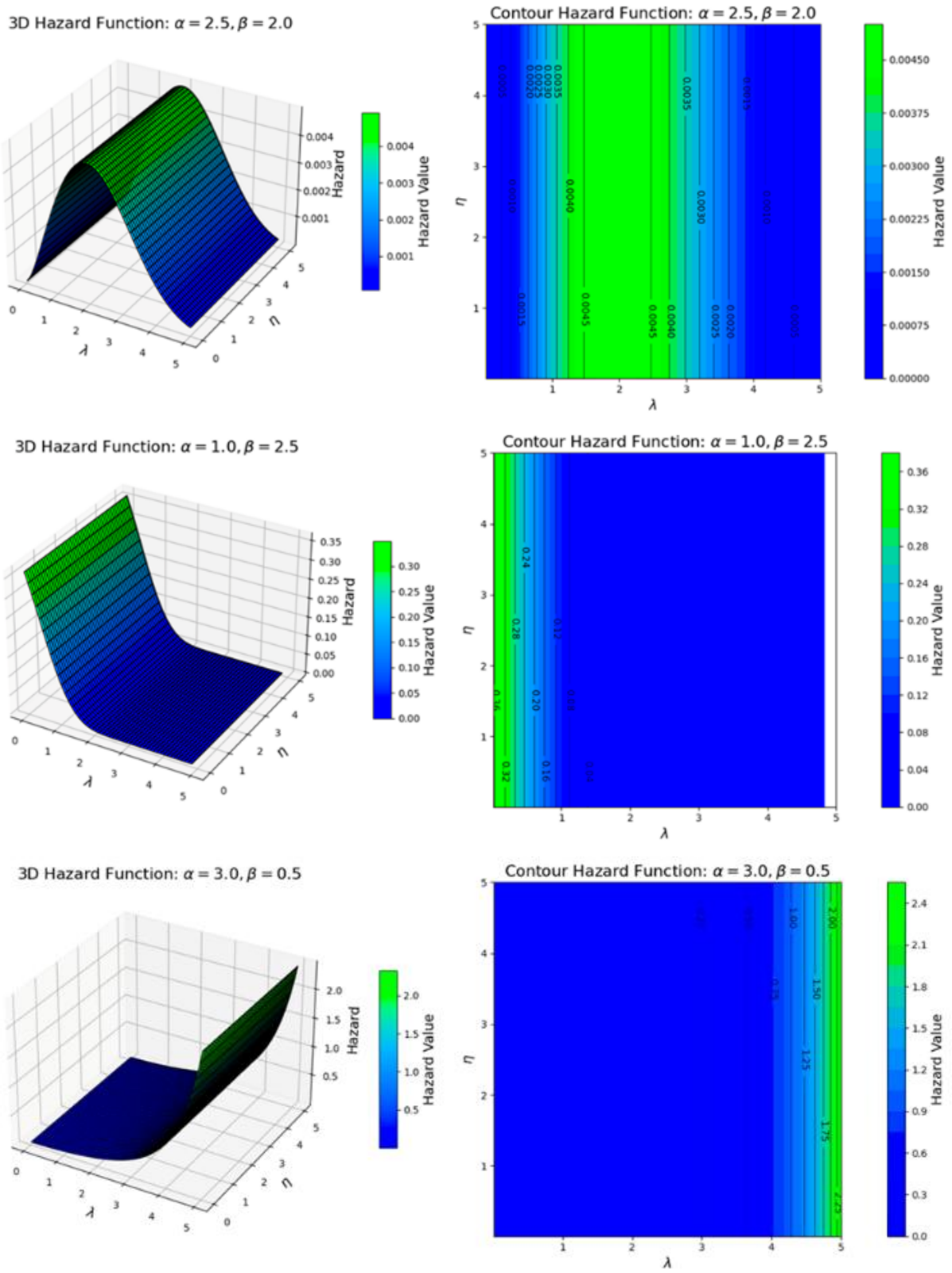

FIGURE 7. 3D hazard function and contour plots of the OBP-Gompertz distribution.

3. Properties of OBP-Gompertz Distribution

This section introduces the key statistical properties of the OBP-Gompertz distribution, including the derivation of moments, moment generating function, Rényi and Tsallis entropies, and stress-strength function. These properties are essential for comprehensive modeling and analysis, providing insights into the distribution's behavior and applications in various fields.

A. Moments

The r^{th} moment of the OBP-Gompertz distribution is expressed as:

$$E\left(X^r\right)=\int_0^\infty x^r f\left(x;\alpha,\beta,\lambda,\eta\right)dx. \tag{15}$$

Substituting the PDF of the OBP-Gompertz distribution from (6) into (15):

$$E\left(X^r\right)=\frac{\lambda\eta}{B(\alpha,\beta)}\int_0^\infty x^r e^{\lambda x}e^{-\eta\left(e^{\lambda x}-1\right)}.\left(1-e^{-\eta\left(e^{\lambda x}-1\right)}\right)^{\alpha-1}.\left(e^{-\eta\left(e^{\lambda x}-1\right)}\right)^{\beta-1}dx. \tag{16}$$

The first four moments of the OBP-Gompertz distribution (for $r=1,2,3,4$) are as follows:

For $r=1$:

$$E\left(X\right)=\frac{\lambda\eta}{B(\alpha,\beta)}\int_0^\infty xe^{\lambda x}e^{-\eta\left(e^{\lambda x}-1\right)}.\left(1-e^{-\eta\left(e^{\lambda x}-1\right)}\right)^{\alpha-1}.\left(e^{-\eta\left(e^{\lambda x}-1\right)}\right)^{\beta-1}dx. \tag{17}$$

For $r=2$:

$$E\left(X^2\right)=\frac{\lambda\eta}{B(\alpha,\beta)}\int_0^\infty x^2e^{\lambda x}e^{-\eta\left(e^{\lambda x}-1\right)}.\left(1-e^{-\eta\left(e^{\lambda x}-1\right)}\right)^{\alpha-1}.\left(e^{-\eta\left(e^{\lambda x}-1\right)}\right)^{\beta-1}dx. \tag{18}$$

For $r=3$ and $r=4$, the process is identical:

$$E\left(X^3\right)=\frac{\lambda\eta}{B(\alpha,\beta)}\int_0^\infty x^3e^{\lambda x}e^{-\eta\left(e^{\lambda x}-1\right)}.\left(1-e^{-\eta\left(e^{\lambda x}-1\right)}\right)^{\alpha-1}.\left(e^{-\eta\left(e^{\lambda x}-1\right)}\right)^{\beta-1}dx. \tag{19}$$

$$E\left(X^4\right)=\frac{\lambda\eta}{B(\alpha,\beta)}\int_0^\infty x^4e^{\lambda x}e^{-\eta\left(e^{\lambda x}-1\right)}.\left(1-e^{-\eta\left(e^{\lambda x}-1\right)}\right)^{\alpha-1}.\left(e^{-\eta\left(e^{\lambda x}-1\right)}\right)^{\beta-1}dx. \tag{20}$$

The variance is then given by:

$$Var\left(X\right)=E\left(X^2\right)-\left(E\left(X\right)\right)^2. \tag{21}$$

The skewness measures the asymmetrical distribution and is given by:

$$Skewness=\frac{E\left(\left(X-\mu\right)^3\right)}{\sigma^3}, \tag{22}$$

where $E\left(\left(X-\mu\right)^3\right)=E\left(X^3\right)-3E\left(X^2\right)E\left(X\right)+2E\left(X\right)^3$, $\mu=E\left(X\right)$ is the mean, and σ^2 is the variance.

The kurtosis measures the tailedness of the distribution and is given by:

$$Kurtosis = \frac{E\left((X-\mu)^4\right)}{\sigma^4}, \tag{23}$$

where $E\left((X-\mu)^4\right) = E\left(X^4\right) - 4E\left(X^3\right)E(X) + 6E\left(X^2\right)\left(E(X)\right)^2 - 3\left(E(X)\right)^4$.

In Table 3, the mean, variance, skewness, and kurtosis of the OBP-Gompertz distribution are presented across various combinations of the parameters $\alpha, \beta, \lambda,$ and η. The table shows how these statistical moments change for different values of $\alpha, \beta, \lambda,$ and η, providing insights into the distribution's behavior.

For the parameters $\alpha = 1.5, \beta = 0.5, \lambda = 0.5,$ and $\eta = 0.5$, the mean is 3.0586, with a variance of 1.8029, skewness of 0.0556, and kurtosis of -0.5474, indicating a moderately spread distribution with slightly positive skewness and a relatively flat shape. As η increases to 1, the mean decreases to 2.1306, and the variance also decreases to 1.1843, while the skewness becomes more positive (0.3085) and the kurtosis is less negative (-0.4553), suggesting a more pronounced peak and slightly more positive asymmetry. As η increases further, the mean continues to decrease, reaching 1.1115 at $\eta = 1.5$, with the variance dropping to 0.4566. The skewness increases to 0.6707, and the kurtosis becomes positive (0.0773), indicating that the distribution is becoming more concentrated around the mean and less spread out. At higher values of λ (1.5 and beyond), the mean, variance, and skewness values all tend to decrease, while kurtosis moves toward a more positive value, signaling a transition toward a more concentrated distribution with a sharper peak. For higher values of α (2.0 and 2.5), the mean continues to decrease, while variance and skewness also show decreasing trends. For instance, when $\alpha = 2.0, \beta = 0.5, \lambda = 0.5,$ and $\eta = 0.5$, the mean is 3.3022, and the variance is 1.5716. As η increases, the mean continues to decrease, and the skewness remains relatively low. This pattern is also visible for higher values of α, where the distribution becomes more concentrated, with lower mean values and higher peak (positive kurtosis) values at higher η values.

The skewness remains positive for most combinations of parameters, but its magnitude increases as η increases, suggesting that the distribution becomes more asymmetric. The kurtosis, in general, shows more negative values at lower values of η, indicating a flatter distribution, but as η increases, the kurtosis becomes positive, reflecting a sharper peak. The trend is consistent across different values of α and β. Overall, the results from Table 3 indicate that as η increases, the OBP-Gompertz distribution tends to become more concentrated around the mean with higher skewness and kurtosis values, especially for higher values of α and β. The distribution exhibits

more pronounced changes in the statistical moments as η increases, suggesting a shift towards a more ordered and less spread-out distribution

The 3D and contour plots in Figs. 8-11 provide a comprehensive view of the OBP-Gompertz distribution's statistical properties under specific parameter constraints. By fixing the values of α and β, we can explore the behavior of the distribution with respect to λ and η. The 3D plots visualize the overall shape of the statistical measure, while the contour plots highlight specific regions of interest and the rate of change. For instance, in Fig. 8, the contour lines reveal how the mean increases with both λ and η, while in Fig. 9, the contour lines show how the variance changes with respect to the parameters. In Fig. 10, the contour lines illustrate how the skewness can be positive or negative depending on the parameter values, highlighting the distribution's flexibility in capturing asymmetry. Similarly, in Fig. 11, the contour lines show how the kurtosis varies with λ and η, indicating the distribution's ability to model different levels of tail weight.

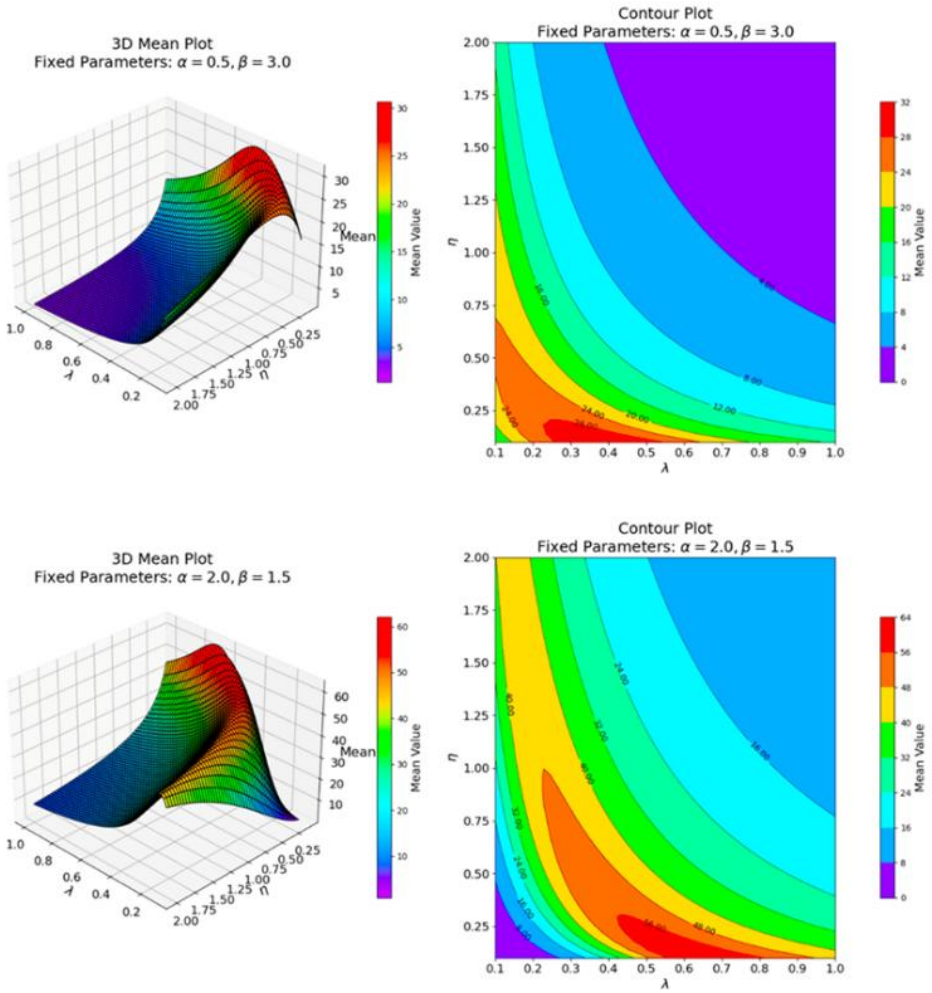

FIGURE 8. 3D mean and contour plots of the OBP-Gompertz distribution.

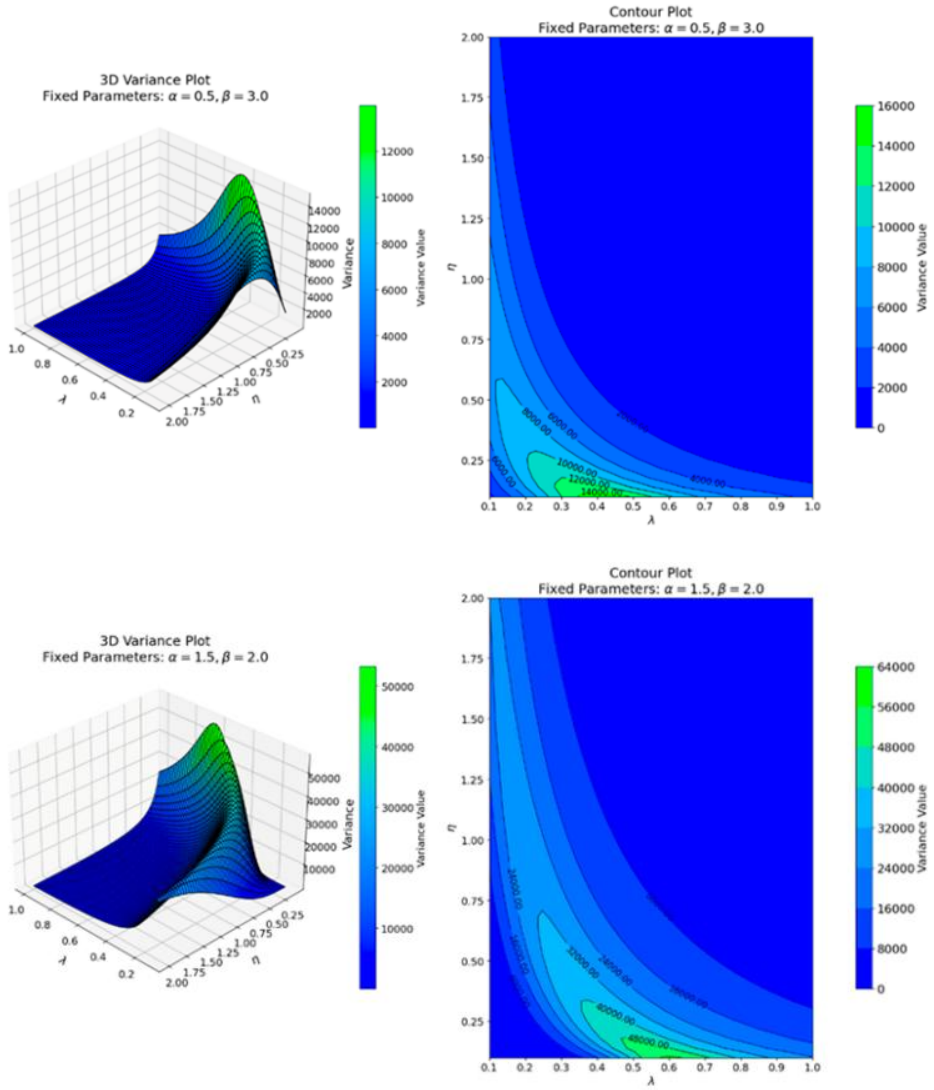

FIGURE 9. 3D variance and contour plots of the OBP-Gompertz distribution.

TABLE 3. The mean, variance, skewness, and kurtosis for the OBP-Gompertz distribution

α	β	λ	η	Mean	Variance	Skewness	Kurtosis
1.5	0.5	0.5	0.5	3.0586	1.8029	0.0556	-0.5474
1.5	0.5	0.5	1	2.1306	1.1843	0.3085	-0.4553
1.5	0.5	0.5	1.5	1.6739	0.8637	0.4678	-0.2859
1.5	1	0.5	0.5	2.2312	1.1992	0.2358	-0.4983
1.5	1	0.5	1	1.4661	0.6854	0.5067	-0.2158
1.5	1	0.5	1.5	1.1115	0.4566	0.6707	0.0773
1.5	1	1	0.5	1.1156	0.2998	0.2358	-0.4983
1.5	1	1	1	0.733	0.1714	0.5067	-0.2158
1.5	1	1	1.5	0.5557	0.1142	0.6707	0.0773
1.5	1	1.5	0.5	0.7437	0.1332	0.2358	-0.4983
1.5	1	1.5	1	0.4887	0.0762	0.5067	-0.2158
1.5	1	1.5	1.5	0.3705	0.0507	0.6707	0.0773
1.5	1.5	0.5	0.5	1.8042	0.8985	0.3588	-0.4032
1.5	1.5	0.5	1	1.1436	0.4689	0.6344	0.0052
1.5	1.5	0.5	1.5	0.8492	0.2954	0.7962	0.3688
1.5	1.5	1	0.5	0.9021	0.2246	0.3588	-0.4032
1.5	1.5	1	1	0.5718	0.1172	0.6344	0.0052
1.5	1.5	1	1.5	0.4246	0.0738	0.7962	0.3688
1.5	1.5	1.5	0.5	0.6014	0.0998	0.3588	-0.4032
1.5	1.5	1.5	1	0.3812	0.0521	0.6344	0.0052
1.5	1.5	1.5	1.5	0.2831	0.0328	0.7962	0.3688
2	0.5	0.5	0.5	3.3022	1.5716	0.0208	-0.427
2	0.5	0.5	1	2.3205	1.0749	0.2574	-0.3884
2	0.5	0.5	1.5	1.8317	0.8018	0.4097	-0.2577
2	1	0.5	0.5	2.4989	1.0787	0.1406	-0.4237
2	1	0.5	1	1.6627	0.6475	0.3971	-0.2464
2	1	0.5	1.5	1.2689	0.4428	0.5547	-0.0218
2	1	1	0.5	1.2495	0.2697	0.1406	-0.4237
2	1	1	1	0.8265	0.1212	0.3971	-0.2464
2	1	1	1.5	0.6118	0.0744	0.5547	-0.0218
2	1	1.5	0.5	0.8679	0.1264	0.1406	-0.4237
2	1	1.5	1	0.5663	0.0704	0.3971	-0.2464
2	1	1.5	1.5	0.4293	0.0456	0.5547	-0.0218
2	1.5	0.5	0.5	2.3489	1.0078	0.2499	-0.3898
2	1.5	0.5	1	1.5551	0.5773	0.4827	-0.0954
2	1.5	0.5	1.5	1.1878	0.3556	0.6423	0.1417
2	1.5	1	0.5	1.2361	0.2154	0.2499	-0.3898
2	1.5	1	1	0.8306	0.0963	0.4827	-0.0954
2	1.5	1	1.5	0.6164	0.0603	0.6423	0.1417
2	1.5	1.5	0.5	0.8687	0.1225	0.2499	-0.3898
2	1.5	1.5	1	0.5772	0.0689	0.4827	-0.0954
2	1.5	1.5	1.5	0.4296	0.0429	0.6423	0.1417

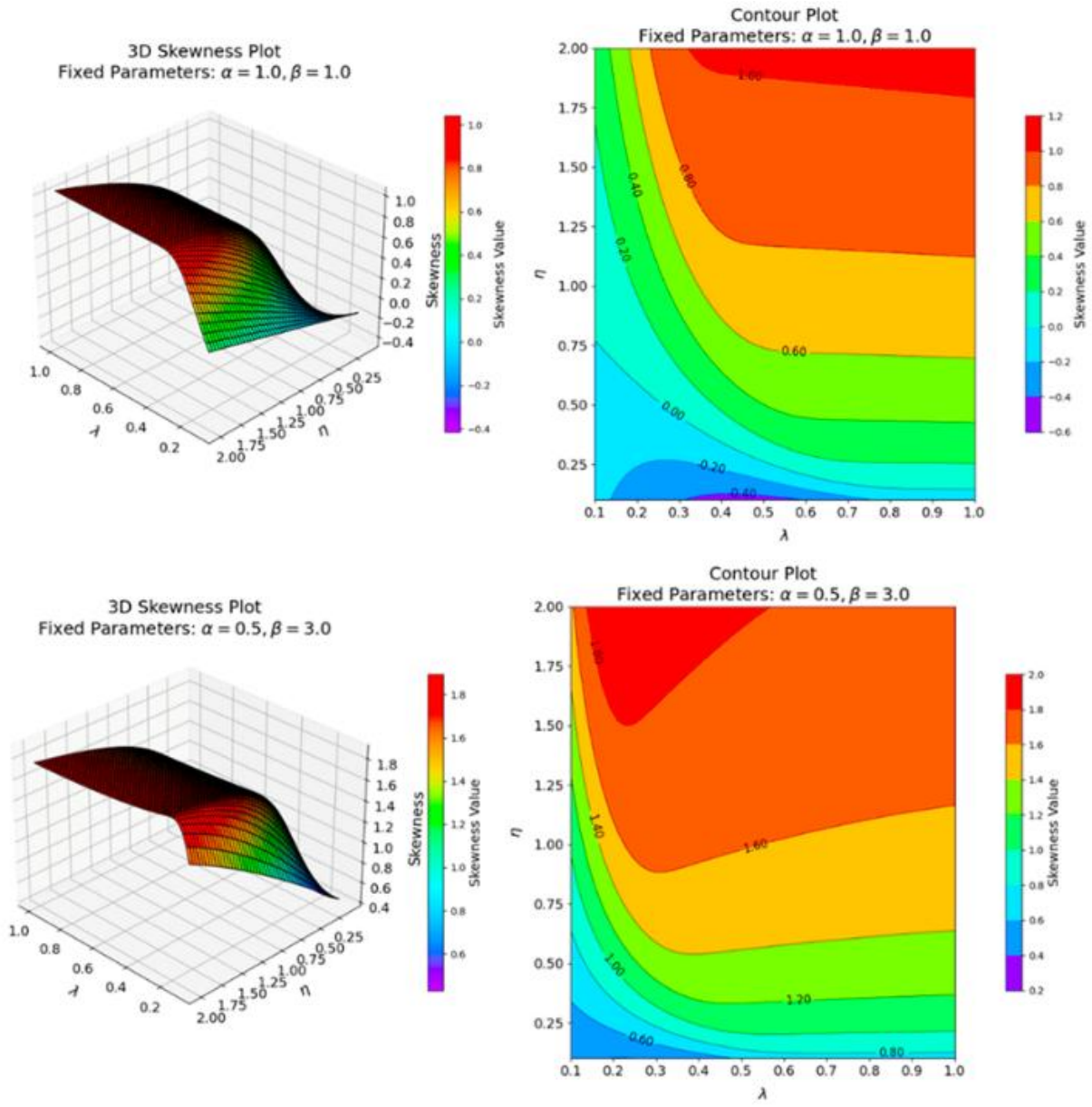

FIGURE 10. 3D skewness and contour plots of the OBP-Gompertz distribution.

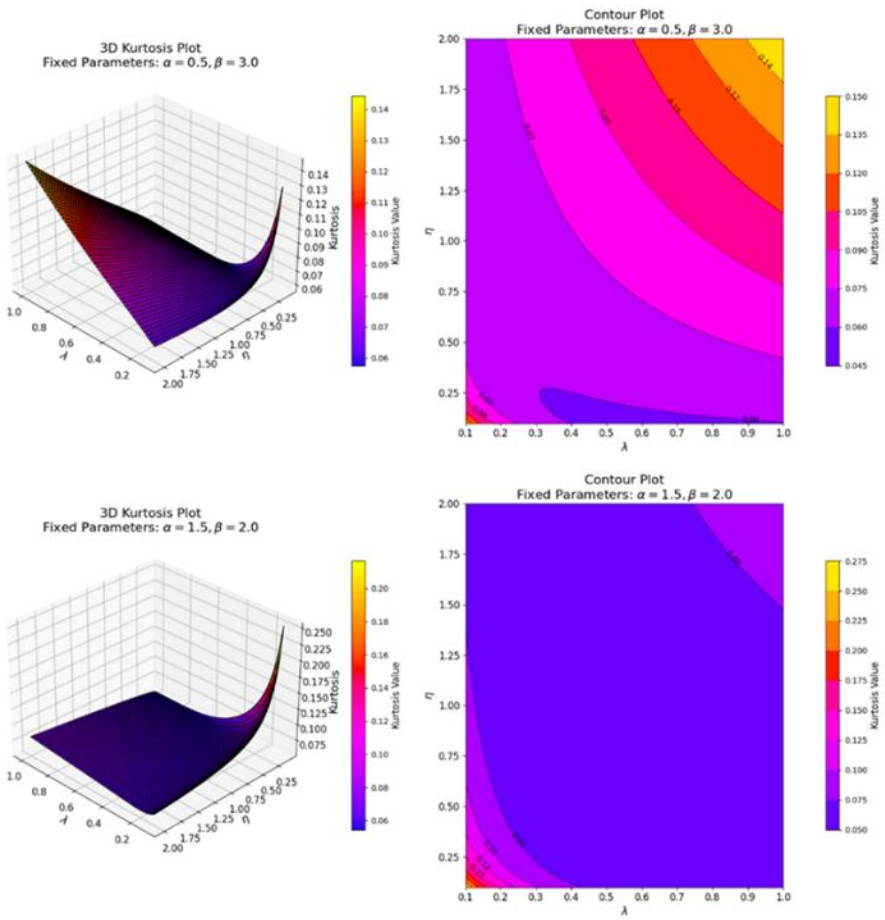

FIGURE 11. 3D kurtosis and contour plots of the OBP-Gompertz distribution.

B. Moment Generating Function

The moment generating function (MGF) is given by:

$$M_X(t) = E\left(e^{tX}\right) = \int_0^{\infty} e^{tx} f(x;\alpha,\beta,\lambda,\eta)\,dx. \tag{24}$$

Substituting the PDF of the OBP-Gompertz distribution from (6) into (24):

$$M_X(t) = \frac{\lambda\eta}{B(\alpha,\beta)} \int_0^{\infty} e^{tx} e^{\lambda x} e^{-\eta\left(e^{\lambda x}-1\right)} \cdot \left(1-e^{-\eta\left(e^{\lambda x}-1\right)}\right)^{\alpha-1} \cdot \left(e^{-\eta\left(e^{\lambda x}-1\right)}\right)^{\beta-1} dx. \tag{25}$$

C. Quantile Function

The quantile function $Q(p)$ of the OBP-Gompertz distribution is defined as the inverse of the CDF in (5). By definition, an inverse function $Q(p)$ must satisfy the conditions outlined by the following functional equation:

$$F\left(Q(p)\right) = p \text{ for every } p \in [0,1]. \tag{26}$$

Using the CDF provided in (5) applies:

$$\frac{1}{B(\alpha,\beta)}\int_0^{M(Q(p))} u^{\alpha-1}(1-u)^{\beta-1}\,du = p. \tag{27}$$

Solving for $Q(p)$ requires inverting $1-e^{-\eta\left(e^{\lambda x}-1\right)} = M(x;\lambda,\eta)$, which gives:

$$Q(p) = \frac{1}{\lambda}\ln\left(1+\frac{1}{\eta}\ln(1-p)\right). \tag{28}$$

D. Rényi and Tsallis Entropy Measures

The Rényi entropy for the OBP-Gompertz distribution is defined as:

$$H_R(q) = \frac{1}{1-q}\ln\int_0^{\infty}\left[f(x;\alpha,\beta,\lambda,\eta)\right]^q dx, \quad q>0,\ q\neq 1. \tag{29}$$

Substituting (6) into (29):

$$H_R(q) = \frac{1}{1-q}\ln\int_0^{\infty}\left[\frac{\lambda\eta e^{\lambda x}e^{-\eta\left(e^{\lambda x}-1\right)}\cdot\left[1-e^{-\eta\left(e^{\lambda x}-1\right)}\right]^{\alpha-1}\cdot\left[e^{-\eta\left(e^{\lambda x}-1\right)}\right]^{\beta-1}}{B(\alpha,\beta)}\right]^q dx. \tag{30}$$

Expanding the q^{th} power and simplifying the exponent (30) becomes:

$$H_R(q) = \frac{1}{1-q}\ln\left(\frac{1}{\left(B(\alpha,\beta)\right)^q}(\lambda\eta)^q.I\right), \tag{31}$$

where $I = \int_0^{\infty} e^{q\lambda x}.e^{-q\beta\eta\left(e^{\lambda x}-1\right)}.\left(1-e^{-\eta\left(e^{\lambda x}-1\right)}\right)^{q(\alpha-1)} dx.$

The Tsallis entropy for the OBP-Gompertz distribution is defined as:

$$H_T(q) = \frac{1}{1-q}\left[1-\int_0^{\infty}\left(f(x;\alpha,\beta,\lambda,\eta)\right)^q dx\right], \quad q>0,\ q\neq 1. \tag{32}$$

Substituting (6) into (32), the Tsallis entropy becomes:

$$H_T(q) = \frac{1}{1-q}\left[1-\int_0^{\infty}\left(\frac{\lambda\eta e^{\lambda x}e^{-\eta\left(e^{\lambda x}-1\right)}\cdot\left[1-e^{-\eta\left(e^{\lambda x}-1\right)}\right]^{\alpha-1}\cdot\left[e^{-\eta\left(e^{\lambda x}-1\right)}\right]^{\beta-1}}{B(\alpha,\beta)}\right)^q dx\right]. \tag{33}$$

Expanding the q^{th} power and simplify the exponent (33) becomes:

$$H_T(q) = \frac{1}{1-q}\left[1-\frac{1}{\left(B(\alpha,\beta)\right)^q}(\eta\lambda)^q\int_0^{\infty} e^{q\lambda x-C\left(e^{\lambda x}-1\right)}.\left(1-e^{-\eta\left(e^{\lambda x}-1\right)}\right)^{q(\alpha-1)} dx\right], \tag{34}$$

where $C = q\eta.\left[1+(\beta-1)\right]$. The Tsallis entropy for the OBP-Gompertz distribution is:

$$H_T(q)=\frac{1}{1-q}\left[1-\frac{(\eta\lambda)^q.I_T}{\left(B(\alpha,\beta)\right)^q}\right], \tag{35}$$

where $I_T=\int_0^\infty e^{q\lambda x-C\left(e^{\lambda x}-1\right)}.\left(1-e^{-\eta\left(e^{\lambda x}-1\right)}\right)^{q(\alpha-1)}dx.$

In Table 4, the Rényi and Tsallis entropy values of the OBP-Gompertz distribution are presented across various parameter combinations $\alpha,\beta,\lambda,$ and η, with the entropies computed for different values of q. The table shows how entropy changes for $q=1.5,q=2.0,$ and $q=2.5$, both for Rényi and Tsallis entropy measures. For $\alpha=1.5,\beta=0.5,$ and $\lambda=0.5$, the entropy values are relatively high. At $q=0.5$, Rényi entropy is 1.6365 and Tsallis entropy is 1.1176, indicating higher uncertainty in the system. As q increases to 1.5, Rényi entropy decreases, reaching 1.5663, while Tsallis entropy drops to 0.6031, reflecting a decrease in entropy as the system moves toward more ordered behavior.

For the same set of parameters, when η increases from 0.5 to 1.5, the entropy values generally decrease, particularly for Tsallis entropy. For example, at $\eta=1.5$, the Rényi entropy for $q=0.5$ is 1.2293, which is smaller than the value at $\eta=0.5$, reflecting a lower level of uncertainty as η increases. This pattern continues for higher values of q, with a more pronounced drop for Tsallis entropy compared to Rényi entropy, suggesting that Tsallis entropy is more sensitive to changes in η. As the parameter α increases, the entropy values exhibit more notable changes. For instance, at $\alpha=1.5,\beta=1.5,$ and $\lambda=0.5$, the Rényi entropy at $q=0.5$ is 1.2447, which decreases to 0.167 as α reaches 2.5, showing a sharp decline in entropy as the shape parameter increases. The corresponding Tsallis entropy shows a similar but slightly smaller decrease. The entropy values demonstrate a consistent trend as the parameters $\alpha,\beta,$ and η increase, the entropy generally decreases, indicating a more ordered or predictable system. However, the Tsallis entropy tends to decrease more significantly than the Rényi entropy, suggesting that Tsallis entropy is more sensitive to the changes in the distribution's shape.

Fig. 12 showcases the Rényi entropy of the OBP-Gompertz distribution in a 3D plot and a contour plot. The contour plot reveals a nuanced relationship between the parameters λ and η. As λ increases, the entropy generally rises, indicating a growing degree of uncertainty or randomness within the system. However, the impact of η is more intricate, demonstrating the distribution's flexibility in capturing a wide range of information-theoretic behaviors. This adaptability makes the OBP-Gompertz distribution a powerful tool for modeling complex systems with varying levels of uncertainty and complexity. Fig. 13 presents the Tsallis entropy of the OBP-Gompertz distribution in both 3D and contour plot formats. The contour plot highlights

the distribution's sensitivity to both λ and η. Increasing λ leads to higher Tsallis entropy, suggesting increased complexity and non-extensivity. Conversely, increasing η tends to decrease the Tsallis entropy, indicating a more ordered and less complex system. This flexibility allows the OBP-Gompertz distribution to accommodate a broad spectrum of real-world systems with varying degrees of non-extensivity and complexity.

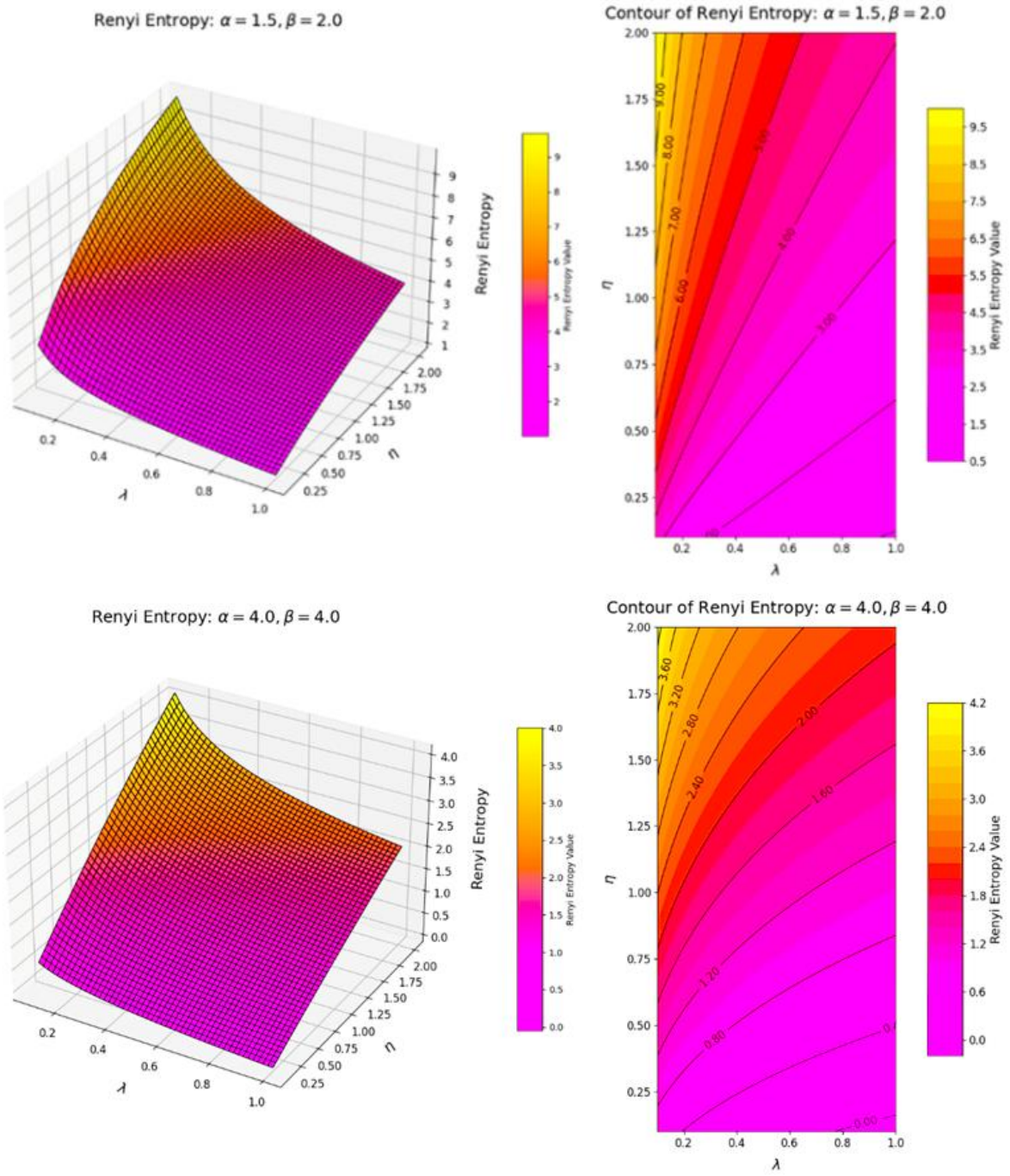

FIGURE 12. 3D Rényi entropy and contour plots of the OBP-Gompertz distribution.

TABLE 4. Rényi and Tsallis entropy measures for the OBP-Gompertz distribution

				$q=1.5$		$q=2.0$		$q=2.5$	
α	β	λ	η	Rényi Entropy	Tsallis Entropy	Rényi Entropy	Tsallis Entropy	Rényi Entropy	Tsallis Entropy
1.5	0.5	0.5	0.5	1.6365	1.1176	1.5963	0.7974	1.5663	0.6031
1.5	0.5	0.5	1	1.4101	1.0118	1.3732	0.7467	1.3461	0.5782
1.5	0.5	0.5	1.5	1.2293	0.9183	1.1908	0.696	1.1631	0.5502
1.5	1	0.5	0.5	1.4234	1.0184	1.3863	0.75	1.3589	0.5798
1.5	1	0.5	1	1.1072	0.8502	1.0678	0.6563	1.0396	0.5265
1.5	1	0.5	1.5	0.8707	0.7059	0.8267	0.5625	0.7955	0.4645
1.5	1	1	0.5	0.7303	0.6118	0.6931	0.5	0.6658	0.4211
1.5	1	1	1	0.414	0.374	0.3747	0.3125	0.3465	0.2702
1.5	1	1	1.5	0.1776	0.1699	0.1335	0.125	0.1023	0.0948
1.5	1	1.5	0.5	0.3248	0.2998	0.2877	0.25	0.2603	0.2155
1.5	1	1.5	1	0.0086	0.0085	-0.0308	-0.0313	-0.059	-0.0617
1.5	1	1.5	1.5	-0.2279	-0.2414	-0.2719	-0.3125	-0.3032	-0.3838
1.5	1.5	0.5	0.5	1.2656	0.9378	1.2286	0.7073	1.2016	0.5567
1.5	1.5	0.5	1	0.8919	0.7196	0.8491	0.5722	0.8187	0.4714
1.5	1.5	0.5	1.5	0.6234	0.5356	0.5747	0.4371	0.5403	0.3702
1.5	1.5	1	0.5	0.5725	0.4978	0.5354	0.4146	0.5085	0.3557
1.5	1.5	1	1	0.1987	0.1892	0.156	0.1444	0.1256	0.1144
1.5	1.5	1	1.5	-0.0697	-0.071	-0.1185	-0.1258	-0.1528	-0.1717
1.5	1.5	1.5	0.5	0.167	0.1602	0.13	0.1219	0.103	0.0955
1.5	1.5	1.5	1	-0.2067	-0.2178	-0.2495	-0.2834	-0.2799	-0.3478
1.5	1.5	1.5	1.5	-0.4752	-0.5364	-0.524	-0.6887	-0.5583	-0.8736
2	0.5	0.5	0.5	1.5667	1.0862	1.5198	0.7813	1.4857	0.5949
2	0.5	0.5	1	1.369	0.9913	1.3257	0.7344	1.2941	0.571
2	0.5	0.5	1.5	1.2067	0.9061	1.1632	0.6875	1.1316	0.5446
2	1	0.5	0.5	1.3768	0.9952	1.3322	0.7361	1.2997	0.5718
2	1	0.5	1	1.1016	0.847	1.0578	0.6528	1.0262	0.5236
2	1	0.5	1.5	0.8886	0.7175	0.8427	0.5694	0.8098	0.4688
2	1	1	0.5	0.6837	0.5791	0.6391	0.4722	0.6066	0.3983
2	1	1	1	0.4084	0.3694	0.3646	0.3056	0.3331	0.2621
2	1	1	1.5	0.1955	0.1863	0.1495	0.1389	0.1167	0.107
2	1	1.5	0.5	0.2782	0.2597	0.2336	0.2083	0.2011	0.1736
2	1	1.5	1	0.003	0.003	-0.0408	-0.0417	-0.0724	-0.0765
2	1	1.5	1.5	-0.21	-0.2214	-0.2559	-0.2917	-0.2888	-0.3615
2	1.5	0.5	0.5	1.2447	0.9266	1.2014	0.6992	1.1698	0.5514
2	1.5	0.5	1	0.9171	0.7356	0.8723	0.582	0.8402	0.4776
2	1.5	0.5	1.5	0.6732	0.5716	0.6252	0.4648	0.5911	0.392
2	1.5	1	0.5	0.5516	0.4821	0.5082	0.3984	0.4767	0.3406
2	1.5	1	1	0.224	0.2119	0.1792	0.1641	0.1471	0.132
2	1.5	1	1.5	-0.0199	-0.02	-0.068	-0.0703	-0.1021	-0.1103
2	1.5	1.5	0.5	0.1461	0.1409	0.1028	0.0977	0.0712	0.0676

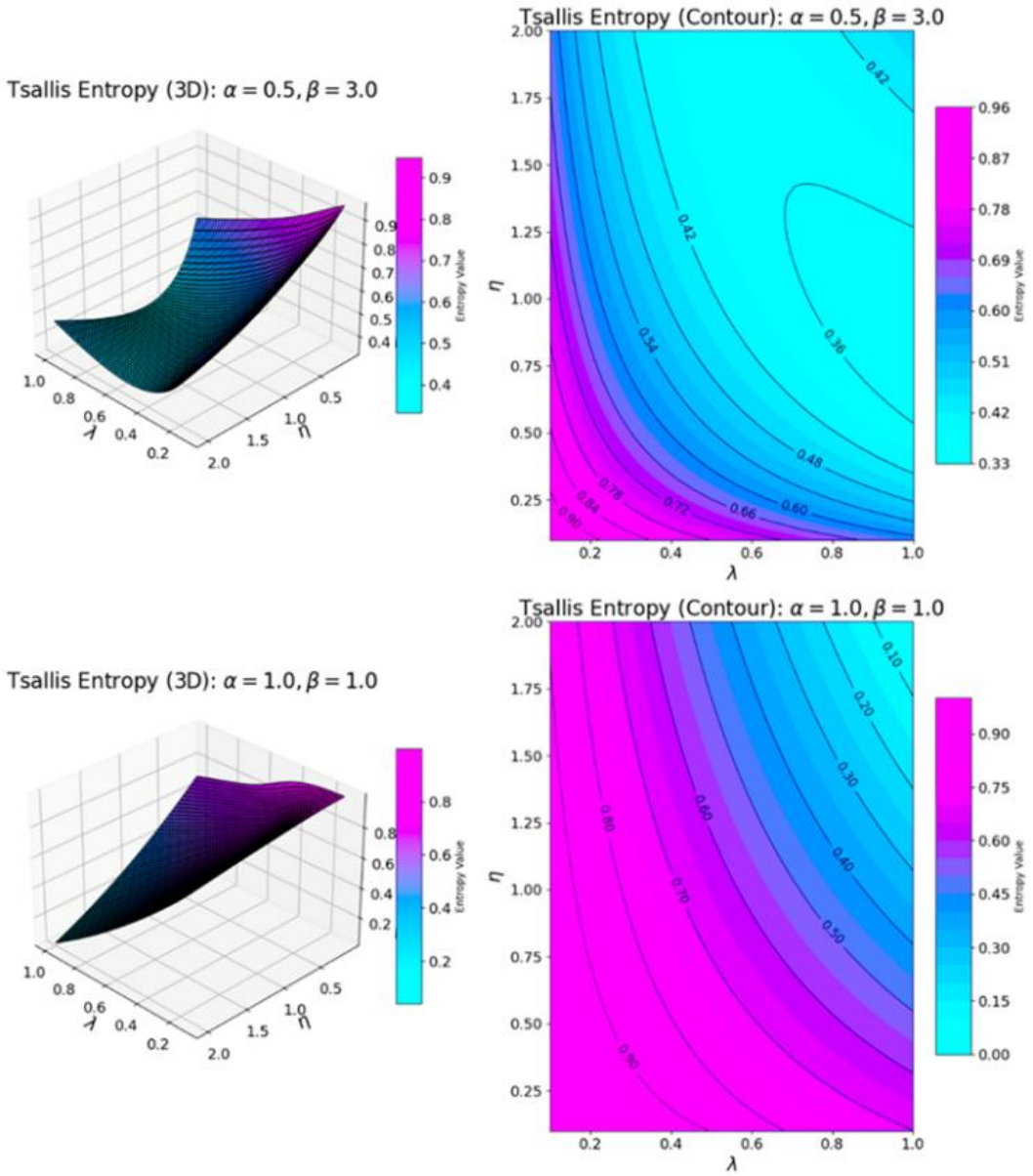

FIGURE 13. 3D Tsallis entropy and contour plots of the OBP-Gompertz distribution.

4. Estimation of Parameter

The maximum likelihood estimation (MLE) is a method used to estimate the parameters of a distribution by maximizing the likelihood function. In this section, we derive the MLEs for the parameters of the OBP-Gompertz distribution.

Suppose we have a sample of size n, denoted by $\{x_1, x_2, ..., x_n\}$. The likelihood function is given by:

$$L(\alpha, \beta, \lambda, \eta) = \prod_{i=1}^{n} f(x_i; \alpha, \beta, \lambda, \eta), \tag{36}$$

where $f(x_i;\alpha,\beta,\lambda,\eta)$ is the PDF of the OBP-Gompertz distribution expressed in (6). Substituting (6) into (36), we have:

$$L(\alpha,\beta,\lambda,\eta)=\frac{1}{\left(B(\alpha,\beta)\right)^n}\prod_{i=1}^{n}\left[\eta\lambda e^{\lambda x_i}e^{-\eta\left(e^{\lambda x_i}-1\right)}.\left(1-e^{-\eta\left(e^{\lambda x_i}-1\right)}\right)^{\alpha-1}.\left(e^{-\eta\left(e^{\lambda x_i}-1\right)}\right)^{\beta-1}\right]. \tag{37}$$

Taking the natural logarithm of the likelihood function to obtain the log-likelihood function:

$$\ell(\alpha,\beta,\lambda,\eta)=-n\ln B(\alpha,\beta)+\sum_{i=1}^{n}\ln\left[\eta\lambda e^{\lambda x_i-\eta\left(e^{\lambda x_i}-1\right)}\right]+(\alpha-1)\sum_{i=1}^{n}\ln\left[1-e^{-\eta\left(e^{\lambda x_i}-1\right)}\right]$$
$$+(\beta-1)\sum_{i=1}^{n}\ln\left[e^{-\eta\left(e^{\lambda x_i}-1\right)}\right]. \tag{38}$$

Upon simplification, we have:

$$\ell(\alpha,\beta,\lambda,\eta)=-n\ln B(\alpha,\beta)+n\ln(\eta\lambda)+\lambda\sum_{i=1}^{n}x_i-\eta\sum_{i=1}^{n}\left(e^{\lambda x_i}-1\right)$$
$$+(\alpha-1)\sum_{i=1}^{n}\ln\left[1-e^{-\eta\left(e^{\lambda x_i}-1\right)}\right]-(\beta-1)\eta\sum_{i=1}^{n}\left(e^{\lambda x_i}-1\right). \tag{39}$$

To find the MLEs, we take partial derivatives of $\ell(\alpha,\beta,\lambda,\eta)$ with respect to $\alpha,\beta,\lambda,$ and η, and set them equal to zero as follows:

$$\frac{\ell(\alpha,\beta,\lambda,\eta)}{\partial\alpha}=-n\left(\psi(\alpha)-\psi(\alpha+\beta)\right)+\sum_{i=1}^{n}\ln\left[1-e^{-\eta\left(e^{\lambda x_i}-1\right)}\right], \tag{40}$$

where $\psi(.)$ is the digamma function.

$$\frac{\ell(\alpha,\beta,\lambda,\eta)}{\partial\beta}=-n\left(\psi(\beta)-\psi(\alpha+\beta)\right)-\eta\sum_{i=1}^{n}\left(e^{\lambda x_i}-1\right), \tag{41}$$

$$\frac{\ell(\alpha,\beta,\lambda,\eta)}{\partial\lambda}=\frac{n}{\lambda}+\sum_{i=1}^{n}x_i-\eta\sum_{i=1}^{n}e^{\lambda x_i}x_i, \tag{42}$$

$$\frac{\ell(\alpha,\beta,\lambda,\eta)}{\partial\eta}=\frac{n}{\eta}-\sum_{i=1}^{n}\left(e^{\lambda x_i}-1\right)+(\alpha-1)\sum_{i=1}^{n}\frac{e^{-\eta\left(e^{\lambda x_i}-1\right)}\left(e^{\lambda x_i}-1\right)}{1-e^{-\eta\left(e^{\lambda x_i}-1\right)}}. \tag{43}$$

Because (40-43) are nonlinear, numerical optimization techniques such as the Newton-Raphson method are required to estimate $\alpha,\beta,\lambda,$ and η.

5. Monte Carlo Simulation

This section presents the results of Monte Carlo simulations conducted to evaluate the performance of the MLE method for estimating the parameters of the OBP-Gompertz distribution across varying sample sizes ($n = 10,20,30,40,50,100,150,200$). The simulations involved generating random samples based on two parameter configurations: Case I ($\alpha = 2.0, \beta = 3.0, \lambda = 0.5, \eta = 1.0$) and Case II $\alpha = 1.0, \beta = 1.0, \lambda = 0.5, \eta = 1.0$. Each experiment was conducted 1000

times to determine the mean estimate, bias, and mean square error (MSE), as presented in Table 5.

In Case I, smaller sample sizes exhibited higher biases and larger MSEs, with bias values ranging from 22.3652 to 0.9848, and MSE values varying from 8177.7443 to 0.9909. These results suggest that for small datasets, the parameter estimates are less stable and more susceptible to variability. However, as the sample size increases, biases diminish, and MSE values decrease substantially, falling to ranges of -1.8190 to -0.9848 for biases and 4.6764 to 0.9909 for MSEs. In Case II, the pattern is similar but with consistently lower levels of bias and MSE across all sample sizes compared to Case I. Biases range from 1.0736 to -0.0081, and MSE values stay between 8.4840 and 0.0230.

The results demonstrate that the OBP-Gompertz distribution and MLE method achieve more accurate and reliable parameter estimates with larger sample sizes. This is evidenced by consistently decreasing bias and MSE, emphasizing the importance of sufficient data for precision. These results are graphically represented in Fig. 14, showing the trends in mean and bias for each parameter across various sample sizes. As expected, both cases demonstrate that MLE performs well for parameter estimation, particularly with larger sample sizes. The biases and means of the parameter estimates exhibit a clear trend of improvement as the sample size increases, especially for the α and η parameters.

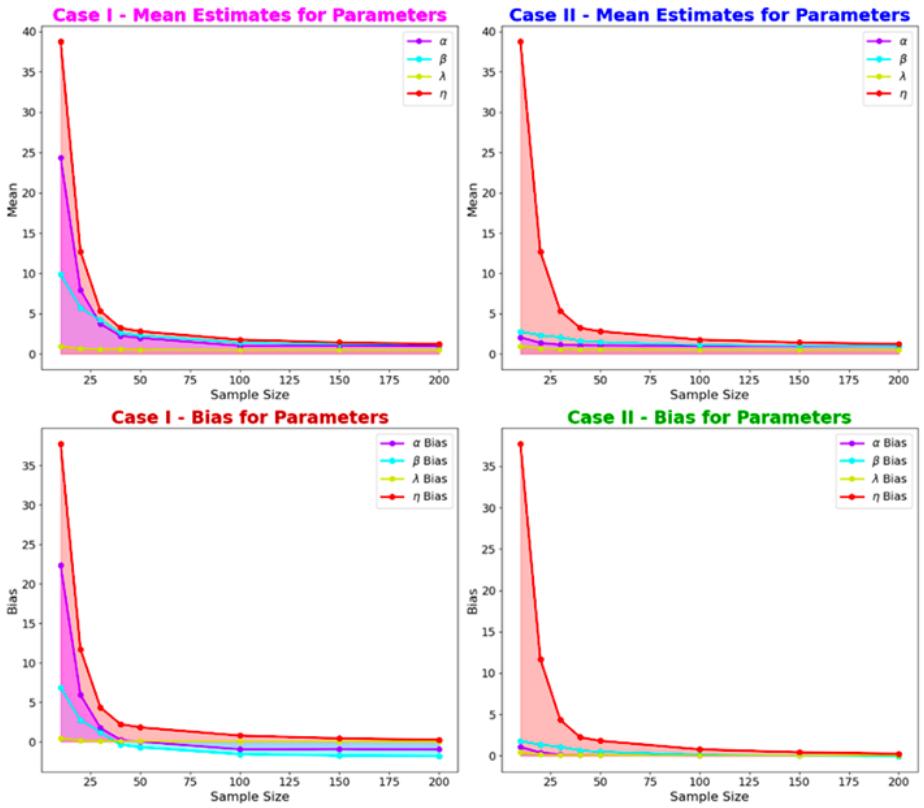

FIGURE 14. Mean and Bias of parameter estimates for Case I and Case II.

TABLE 5. Simulation results for the OBP-Gompertz distribution for Case I and Case II

			Case I $\alpha = 2.0, \beta = 3.0, \lambda = 0.5, \eta = 1.0$			Case II $\alpha = 1.0, \beta = 1.0, \lambda = 0.5, \eta = 1.0$		
η		Estimate	Mean	Bias	MSE	Mean	Bias	MSE
		$\hat{\alpha}$	24.365	22.365	181.74	2.0736	1.0736	8.4840
10		$\hat{\beta}$	9.8830	6.8830	414.70	2.7921	1.7921	19.070
		$\hat{\lambda}$	0.9571	0.4571	1.3444	0.9731	0.4731	1.1425
		$\hat{\eta}$	38.755	37.755	177.50	3.2003	2.2003	20.933
		$\hat{\alpha}$	7.9326	5.9326	145.24	1.3866	0.3866	2.0857
20		$\hat{\beta}$	5.7245	2.7245	183.03	2.3509	1.3509	14.374
		$\hat{\lambda}$	0.6567	0.1567	0.2387	0.6954	0.1954	0.2641
		$\hat{\eta}$	12.707	11.707	119.05	2.8758	1.8758	17.546
		$\hat{\alpha}$	3.7455	1.7455	119.36	1.1588	0.1588	0.7239
30		$\hat{\beta}$	4.2181	1.2181	120.07	2.1042	1.1042	11.447
		$\hat{\lambda}$	0.6064	0.1064	0.1520	0.6227	0.1227	0.1493
		$\hat{\eta}$	5.3459	4.3459	107.23	2.3904	1.3904	12.385
		$\hat{\alpha}$	2.2626	0.2626	116.93	1.0966	0.0966	0.2097
40		$\hat{\beta}$	2.6233	-0.3767	38.081	1.6428	0.6428	7.3262
		$\hat{\lambda}$	0.6053	0.1053	0.1061	0.5875	0.0875	0.1018
		$\hat{\eta}$	3.2367	2.2367	100.90	2.4095	1.4095	11.843
		$\hat{\alpha}$	1.9993	-0.0007	115.46	1.0750	0.0750	0.1785
50		$\hat{\beta}$	2.3068	-0.6932	25.596	1.4994	0.4994	6.0198
		$\hat{\lambda}$	0.5567	0.0567	0.0810	0.5675	0.0675	0.0722
		$\hat{\eta}$	2.8162	1.8162	92.681	2.5120	1.5120	12.379
		$\hat{\alpha}$	1.0272	-0.9728	1.0202	1.0172	0.0172	0.0460
100		$\hat{\beta}$	1.4113	-1.5887	6.6439	1.1149	0.1149	2.0752
		$\hat{\lambda}$	0.5270	0.0270	0.0353	0.5412	0.0412	0.0308
		$\hat{\eta}$	1.7788	0.7788	31.110	2.0629	1.0629	8.1189
		$\hat{\alpha}$	1.0516	-0.9484	1.0021	1.0245	0.0245	0.0332
150		$\hat{\beta}$	1.2333	-1.7667	4.8291	1.0401	0.0401	1.4342
		$\hat{\lambda}$	0.5240	0.0240	0.0203	0.5257	0.0257	0.0196
		$\hat{\eta}$	1.4297	0.4297	31.783	1.8972	0.8972	6.5494
		$\hat{\alpha}$	1.0152	-0.9848	0.9909	0.9919	-0.0081	0.0230
200		$\hat{\beta}$	1.1810	-1.8190	4.6764	0.9643	-0.0357	0.6343
		$\hat{\lambda}$	0.5098	0.0098	0.0157	0.5351	0.0351	0.0171
		$\hat{\eta}$	1.2490	0.2490	6.3406	1.7558	0.7558	5.8491

6. Real Data Application

In this section, we demonstrate the practical utility of the OBP-Gompertz distribution by applying it to analyze COVID-19 mortality rate datasets from China, the Netherlands, and Nepal. Statistical distribution models like the OBP-Gompertz distribution are instrumental in healthcare analytics, providing insights into patterns of disease progression, mortality rates, and other critical metrics. These models enable healthcare professionals to make data-driven decisions, optimize resource allocation, and devise effective public health strategies. In the subsequent sections, we present a detailed analysis of the datasets, comparing the performance of the OBP-Gompertz distribution to other competing models. The results highlight the superior fit of the OBP-Gompertz distribution and its ability to accurately capture the intricacies of the mortality data.

I. First Dataset: COVID-19 Mortality Rate in China

The first dataset represents the COVID-19 mortality rates in China, as reported by Alghamdi and Abd El-Raouf [72]. It consists of 66 observations, capturing mortality rates over a specific period. The data is given as:

8, 16, 15, 24, 26, 26, 38, 43, 46, 45, 57, 64, 65, 73, 73, 86, 89, 97, 108, 97, 146, 121, 143, 142, 105, 98, 136, 114, 118, 109, 97, 150, 71, 52, 29, 44, 47, 35, 42, 31, 38, 31, 30, 28, 27, 22, 17, 22, 11, 7, 13, 10, 14, 13, 11, 8, 3, 7, 6, 9, 7, 4, 6, 5, 3, 5.

II. Second Dataset: COVID-19 Mortality Rate in the Netherlands

The second dataset represents the COVID-19 mortality rates in the Netherlands, as reported Alghamdi and Abd El-Raouf [72]. It consists of 30 observations, reflecting mortality rates over a specific period. The data is given as:

14.918, 10.656, 12.274, 10.289, 10.832, 7.099, 5.928, 13.211, 7.968, 7.584, 5.555, 6.027, 4.097, 3.611, 4.960, 7.498, 6.940, 5.307, 5.048, 2.857, 2.254, 5.431, 4.462, 3.883, 3.461, 3.647, 1.974, 1.273, 1.416, 4.235.

III. Third Dataset: COVID-19 Mortality Rate in Nepal

The third dataset represents the COVID-19 mortality rates in Nepal, as reported by Alghamdi and Abd El-Raouf [72]. It consists of 153 observations, capturing mortality rates over a specific timeframe. The data is given as:

2, 2, 2, 2, 2, 2, 3, 2, 3, 3, 4, 2, 5, 5, 3, 2, 4, 4, 8, 4, 4, 3, 2, 3, 7, 6, 6, 11, 9, 3, 8, 7, 11, 8, 12, 12, 14, 7, 11, 12, 6, 14, 9, 9, 11, 6, 6, 5, 5, 14, 9, 15, 11, 8, 4, 7, 11, 10, 16, 2, 7, 17, 6, 8, 10, 4, 10, 7, 11, 11, 8, 7, 19, 9, 15, 12, 10, 14, 22, 9, 18, 12, 19, 21, 12, 12, 18, 8, 26, 21, 17, 13, 5, 15, 14, 11, 17, 16, 17, 23, 24, 20, 30, 18, 18, 17, 21, 18, 22, 26, 15, 13, 13, 6, 9, 17, 12, 17, 22, 7, 16, 16, 24, 28, 23, 23, 19, 25, 29, 21, 9, 13, 16, 10, 17, 20, 23, 14, 12, 11, 15, 9, 18, 14, 13, 6, 16, 12, 11, 7, 3, 5, 5.

IV. Numerical and Graphical Descriptions of Three Datasets

This subsection provides a detailed numerical and graphical summary of the COVID-19 mortality datasets from China, the Netherlands, and Nepal. The statistical summaries highlight key measures of central tendency, variability, and distribution, while the visualizations offer an in-depth view of the data's characteristics. The COVID-19 mortality data statistical characteristics are summarized in Table 6 and visually analyzed in Figs. 15–17 for China, the Netherlands, and Nepal, respectively.

The dataset from China exhibits a median of 33.00 and a mean of 49.74. The first and third quartiles are 13.00 and 82.75, respectively, indicating a wide range in the data. The minimum value is 3.00, and the maximum is 150.00, resulting in a range of 147. The standard deviation of 43.873 reflects high variability. The skewness of 0.8176 indicates a moderately right-skewed distribution, while the kurtosis of -0.6235 suggests a flatter-than-normal distribution. The dataset from the Netherlands shows a median of 5.369 and a mean of 6.157. The first and third quartiles are 3.706 and 7.562, respectively. The data ranges from 1.273 to 14.918, yielding a range of 13.645.

The standard deviation is 3.5333, indicating moderate variability. A skewness value of 0.7926 suggests slight right skewness, and a kurtosis of -0.2401 points to a nearly normal distribution with slightly flat tails. The dataset from Nepal has a median of 11.00 and a mean of 11.61. The first quartile is 6.00, and the third quartile is 16.00. The minimum and maximum values are 2.00 and 30.00, respectively, resulting in a range of 28. The standard deviation of 6.7591 indicates moderate variability. The skewness of 0.5034 points to slight right skewness, and the kurtosis of -0.4855 reflects a moderately flat-tailed distribution.

To complement the numerical descriptions, various visualization techniques were employed to analyze the datasets, including histograms with kernel density plots, box plots, violin plots, strip plots, and CDF plots. These visualizations provide a comprehensive understanding of the data distributions and characteristics. In Fig. 15, the histogram and kernel density plot highlight a right-skewed distribution with most values concentrated at the lower end and a few outliers extending to the right. The box plot shows potential outliers, while the violin plot provides a detailed view of data density. The strip plot reveals individual observations, and the CDF illustrates cumulative probabilities, indicating a relatively low average mortality rate with some higher values. In Fig. 16, the histogram and kernel density plot for the Netherlands show a slight right skew. The box plot highlights the median and outliers, and the violin plot emphasizes distribution symmetry. The strip plot identifies individual clusters, while the CDF plot provides a cumulative perspective of the data. In Fig. 17, the histogram and kernel density plot display a right-skewed distribution with a higher concentration of lower mortality rates. The box plot identifies the median and potential outliers, and the violin plot gives additional insight

into the distribution's shape. The strip plot and CDF plot provide clarity on individual data points and cumulative trends.

TABLE 6. Summary of the COVID-19 mortality data from China, the Netherlands, and Nepal

Statistics	China	Netherlands	Nepal
Number	66	30	153
Sum	3283	184.695	1777
Median	33.00	5.369	11.00
Mean	49.74	6.157	11.61
First quartile	13.00	3.706	6.00
Third quartile	82.75	7.562	16.00
Std deviation	43.873	3.533312	6.75913
Range	147	13.645	28
Minimum	3.00	1.273	2.00
Maximum	150.00	14.918	30.00
Skewness	0.8176036	0.7926217	0.5033522
Kurtosis	-0.6235147	-0.2401387	-0.485478

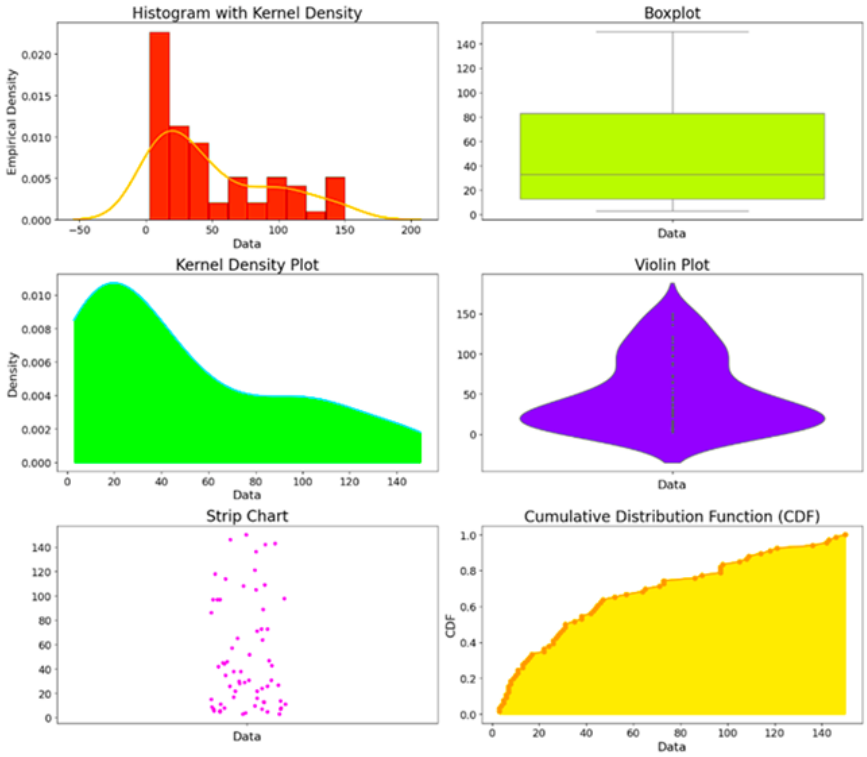

FIGURE 15. Basic non-parametric plots for the COVID-19 mortality rate in China.

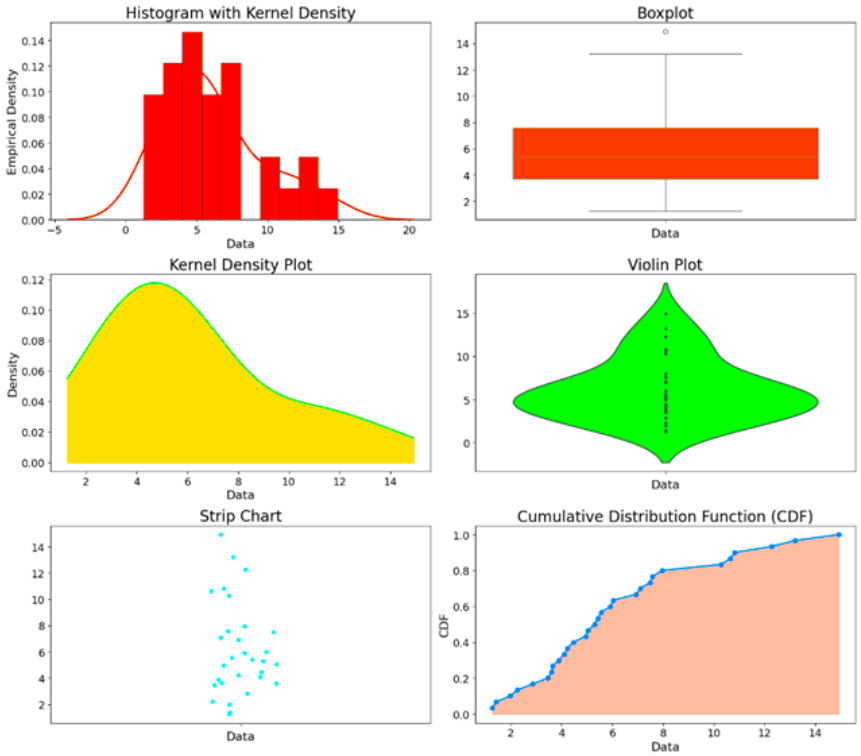

FIGURE 16. Basic non-parametric plots for the COVID-19 mortality rate in the Netherlands.

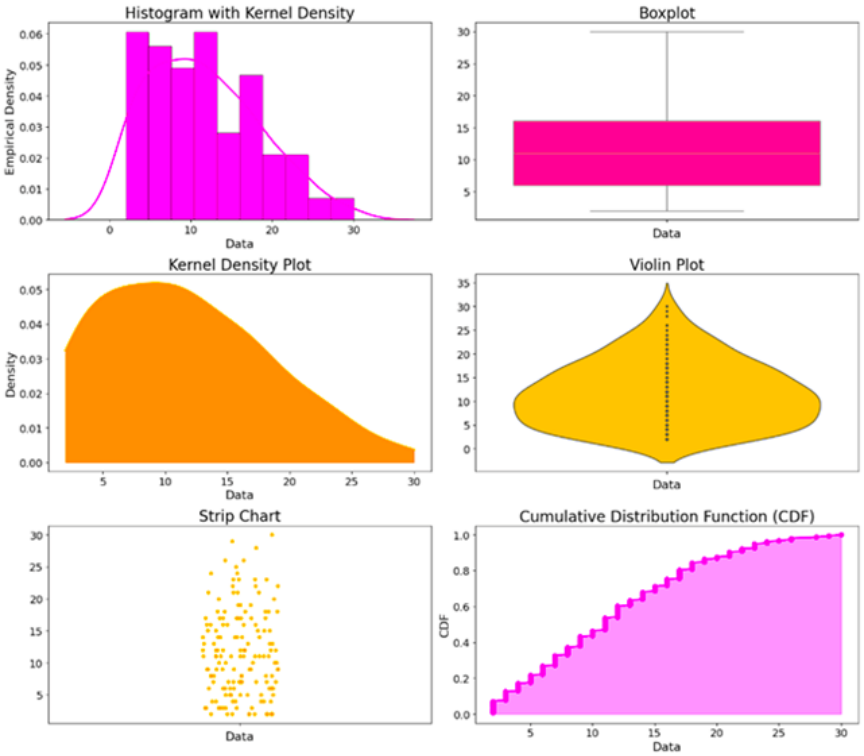

FIGURE 17. Basic non-parametric plots for the COVID-19 mortality rate in Nepal.

V. Model Comparison and Evaluation

The proposed OBP-Gompertz distribution was evaluated against several established models, including the generalized Gompertz (G-Gompertz) distribution by El-Gohary, et al. [52], the Weighted Exponential-Gompertz (WE-Gompertz) distribution by Abd El-Bar and Ragab [73], the Beta-Gompertz distribution by Jafari, et al. [58], and the Gamma-Gompertz distributions by Shama, et al. [74]. The models were assessed using statistical measures such as log-likelihood (LL), Akaike Information Criterion (AIC) and Bayesian Information Criterion (BIC). The results, as shown in Tables 7–9, demonstrate that the OBP-Gompertz distribution consistently outperformed the competing models for COVID-19 mortality data from China, the Netherlands, and Nepal. It achieved the highest log-likelihood values and the lowest AIC and BIC values, indicating its superior fit to the data [75]. While the Beta-Gompertz and G-Gompertz models provided moderately good fits, they incurred higher complexity penalties, reducing their efficiency. In contrast, the WE-Gompertz and Gamma-Gompertz models showed weaker performance, highlighting their limitations in modeling these datasets.

For the China dataset (Table 7), the OBP-Gompertz model demonstrated a highly flexible and accurate fit, achieving optimal values for all the performance metrics. Similarly, for the Netherlands dataset (Table 8), the OBP-Gompertz model maintained its superiority by capturing both central tendencies and tail behaviors effectively. The Beta-Gompertz and G-Gompertz models showed moderate performance across these datasets, while the WE-Gompertz and Gamma-Gompertz models failed to adequately capture the distributional characteristics. For the Nepal dataset (Table 9), the OBP-Gompertz model once again excelled, providing the most accurate and parsimonious fit. Figs. 18–20 provide visual confirmation of these results, showing density plots where the OBP-Gompertz model closely aligns with the empirical data across all datasets. This alignment further validates the model's ability to represent the mortality rate distributions effectively. Overall, the OBP-Gompertz distribution emerges as the most reliable and robust model for these datasets.

TABLE 7. Performance comparison of competing models for COVID-19 from China

Models	Estimates	LL	AIC	BIC
OBP-Gompertz	$\hat{\alpha} = 6.0462$ $\hat{\beta} = 3.3546$ $\hat{\lambda} = 3.6453$ $\hat{\eta} = 1.4532$	-120.456	248.934	256.823
G-Gompertz	$\hat{\lambda} = 3.5644$ $\hat{c} = 0.4536$ $\hat{\theta} = 7.3645$	-128.678	265.343	271.891
WE-Gompertz	$\hat{\lambda} = 6.4657$ $\hat{\sigma} = 1.4536$	-132.230	272.466	278.501
Beta-Gompertz	$\hat{\alpha} = 6.5640$ $\hat{\beta} = 2.6751$ $\hat{\theta} = 1.4567$ $\hat{\gamma} = 0.4531$	-125.894	261.7878	268.340
Gamma-Gompertz	$\hat{\alpha} = 4.6745$ $\hat{\lambda} = 0.6753$ $\hat{\theta} = 0.3421$	-129.341	266.6819	272.56

TABLE 8. Performance comparison of competing models for COVID-19 from the Netherlands

Models	Estimates	LL	AIC	BIC
OBP-Gompertz	$\hat{\alpha} = 6.0462$ $\hat{\beta} = 3.3546$ $\hat{\lambda} = 3.6453$ $\hat{\eta} = 1.4532$	-120.456	248.934	256.823
G-Gompertz	$\hat{\lambda} = 3.5644$ $\hat{c} = 0.4536$ $\hat{\theta} = 7.3645$	-128.678	265.343	271.891
WE-Gompertz	$\hat{\lambda} = 6.4657$ $\hat{\sigma} = 1.4536$	-132.230	272.466	278.501
Beta-Gompertz	$\hat{\alpha} = 6.5640$ $\hat{\beta} = 2.6751$ $\hat{\theta} = 1.4567$ $\hat{\gamma} = 0.4531$	-125.894	261.787	268.340
Gamma-Gompertz	$\hat{\alpha} = 4.6745$ $\hat{\lambda} = 0.6753$ $\hat{\theta} = 0.3421$	-129.341	266.681	272.560

TABLE 9. Performance comparison of competing models for COVID-19 from Nepal

Models	Estimates	LL	AIC	BIC
OBP-Gompertz	$\hat{\alpha} = 3.5764$ $\hat{\beta} = 2.4561$ $\hat{\lambda} = 1.0453$ $\hat{\eta} = 5.8564$	-125.504	255.057	262.501
G-Gompertz	$\hat{\lambda} = 4.5632$ $\hat{c} = 2.8663$ $\hat{\theta} = 2.4658$	-130.801	265.610	273.119
WE-Gompertz	$\hat{\lambda} = 5.9045$ $\hat{\sigma} = 3.7583$	-132.504	269.850	276.594
Beta-Gompertz	$\hat{\alpha} = 1.4653$ $\hat{\beta} = 3.7684$ $\hat{\theta} = 2.7659$ $\hat{\gamma} = 1.9563$	-129.563	263.751	270.451
Gamma-Gompertz	$\hat{\alpha} = 6.8670$ $\hat{\lambda} = 1.6574$ $\hat{\theta} = 2.6701$	-131.850	267.029	274.023

7. CONCLUSION

This study introduces the Odd Beta Prime-Gompertz (OBP-Gompertz) distribution, a flexible extension of the traditional Gompertz model. The OBP-Gompertz distribution demonstrates superior flexibility and surpasses the limitations of the Gompertz model by effectively capturing a wider range of data behaviors. It accommodates diverse density shapes, including right-skewed, left-skewed, heavy-tailed, and light-tailed distributions, and exhibits versatile hazard rate functions, such as increasing, decreasing, bathtub-shaped, and inverted bathtub-shaped curves. These characteristics make the OBP-Gompertz distribution well-suited for modeling complex mortality data observed in real-world scenarios. The paper investigates key structural properties of the OBP-Gompertz distribution, including moments, the quantile function, and the generating function. We explore parameter estimation using maximum likelihood estimation and validate its performance through comprehensive simulation studies.

The practical applicability of the OBP-Gompertz distribution is demonstrated through its application to COVID-19 mortality data from China, the Netherlands, and Nepal. In all cases, the OBP-Gompertz model demonstrates superior adaptability and effectiveness compared to competing models, as evidenced by improved goodness-of-fit measures. These findings highlight the OBP-Gompertz distribution as a valuable tool for researchers and practitioners in various fields. It has the potential to significantly improve the accuracy and reliability of statistical modeling in survival analysis, reliability studies, and epidemiological research.

Future research directions include investigating the OBP-Gompertz distribution applications in regression analysis, investigating its properties under different censoring and truncation schemes.

Conflicts of Interest: The authors declare that there are no conflicts of interest regarding the publication of this paper.

References

[1] I.E. Ragab, H. Daud, A.A. Suleiman, N. Alsadat, V.B. Nagarjuna, M. Elgarhy, Type Ii Topp-Leone Exponentiated Gamma Distribution with Application to Breaking Stress Data, J. Radiat. Res. Appl. Sci. 17 (2024), 101045. https://doi.org/10.1016/j.jrras.2024.101045.

[2] A.A. Alahmadi, R.A. ZeinEldin, O. Albalawi, M.M. Badr, T.A.A. Abdelfadel, A.W. Shawki, Modified Kies Power Lomax Model with Applications in Different Sciences, J. Radiat. Res. Appl. Sci. 18 (2025), 101239. https://doi.org/10.1016/j.jrras.2024.101239.

[3] Y. Yu, Y. Jia, M.A. Alshahrani, O.A. Alamri, H. Daud, J.G. Dar, A.A. Suleiman, Adopting a New Sine-Induced Statistical Model and Deep Learning Methods for the Empirical Exploration of the Music and Reliability Data, Alex. Eng. J. 104 (2024), 396-408. https://doi.org/10.1016/j.aej.2024.07.104.

[4] L.A. Al-Essa, M. Muhammad, M.H. Tahir, B. Abba, J. Xiao, F. Jamal, A New Flexible Four Parameter Bathtub Curve Failure Rate Model, and Its Application to Right-Censored Data, IEEE Access 11 (2023), 50130-50144. https://doi.org/10.1109/access.2023.3276904.

[5] M.I.A. Araibi, A.A. Mir, I. Elbatal, E.M. Almetwally, C. Tanış, E. Ozkan, A.M. Gemeay, A New Alternative to the Log-Kumaraswamy Distribution: Properties, Estimation, and Fitting Data, Int. J. Anal. Appl. 23 (2025), 174. https://doi.org/10.28924/2291-8639-23-2025-174.

[6] U. Panitanarak, A.I. Ishaq, A.A. Suleiman, H. Daud, N.S.S. Singh, A.U. Usman, N. Alsadat, M. Elgarhy, A New Beta Distribution with Interdisciplinary Data Analysis, AIMS Math. 10 (2025), 8495-8527. https://doi.org/10.3934/math.2025391.

[7] N. Alsadat, A.S. Hassan, M. Elgarhy, C. Chesneau, R.E. Mohamed, An Efficient Stress–strength Reliability Estimate of the Unit Gompertz Distribution Using Ranked Set Sampling, Symmetry 15 (2023), 1121. https://doi.org/10.3390/sym15051121.

[8] T.N. Sindhu, A. Shafiq, M.B. Riaz, T.A. Abushal, H. Ahmad, E.M. Almetwally, S. Askar, Introducing the New Arcsine-Generator Distribution Family: An In-Depth Exploration with an Illustrative

Example of the Inverse Weibull Distribution for Analyzing Healthcare Industry Data, J. Radiat. Res. Appl. Sci. 17 (2024), 100879. https://doi.org/10.1016/j.jrras.2024.100879.

[9] A.A. Osi, G.S.S. Abdalla, N.S. Sawaran Singh, A.A. Suleiman, Advancing Lifetime Data Modeling via the Marshall-Olkin Cosine Topp-Leone Distribution Family, Comput. J. Math. Stat. Sci. (2025). https://doi.org/10.21608/cjmss.2025.374786.1155.

[10] C.M. Dalah, V. Singh, I. Abdullahi, A. Suleiman, The Study of HIV/AIDS Trend in Yobe State for the Prescribed Period (1999–2019), Int. J. Stat. Appl. 10 (2020), 10-16.

[11] H. Daud, A.S. Mohammed, A.I. Ishaq, B. Abba, Y. Zakari, J. Abdullahi, D.A. Shobanke, A.A. Suleiman, Modeling and Prediction of Exchange Rates Using Topp-Leone Burr Type X, Machine Learning and Deep Learning Models, Eur. J. Stat. 4 (2024), 11. https://doi.org/10.28924/ada/stat.4.11.

[12] L.P. Sapkota, V. Kumar, G. Tekle, H. Alrweili, M.S. Mustafa, M. Yusuf, Fitting Real Data Sets by a New Version of Gompertz Distribution, Mod. J. Stat. 1 (2025), 25-48. https://doi.org/10.64389/mjs.2025.01109.

[13] U. Danjuma Maiwada, R. Yusuf Zakari, A.A. Janisar, Distribution Function-Driven Handover Solutions for 5G Mobile Networks, J. Stat. Sci. Comput. Intell. 1 (2025), 46-60. https://doi.org/10.64497/jssci.1.

[14] A.A. Suleiman, H. Daud, A.I. Ishaq, R. Sokkalingam, S.A. Suleiman, et al. Extension of the Log-Logistic Distribution for Groundwater Analysis and Potability Prediction Using Machine Learning Models, in: Proceedings of the 5th International Electronic Conference on Applied Sciences, 2024, MDPI, Basel, Switzerland, 2024.

[15] U. Panitanarak, A. Ismail Ishaq, A. Adewole Abiodun, H. Daud, A. Abubakar Suleiman, A New Maxwell-Log Logistic Distribution and Its Applications for Mortality Rate Data, J. Niger. Soc. Phys. Sci. 7 (2025), 1976. https://doi.org/10.46481/jnsps.2025.1976.

[16] Q.N. Husain, A.S. Qaddoori, N.A. Noori, K.N. Abdullah, A.A. Suleiman, O.S. Balogun, New Expansion of Chen Distribution According to the Nitrosophic Logic Using the Gompertz Family, Innov. Stat. Probab. 1 (2025), 60-75. https://doi.org/10.64389/isp.2025.01105.

[17] U. Panitanarak, A.I. Ishaq, A. Usman, I.A. Sadiq, A.S. Mohammed, The Modified Sine Distribution and Machine Learning Models for Enhancing Crude Oil Production Prediction, J. Stat. Sci. Comput. Intell. 1 (2025), 29-45. https://doi.org/10.64497/jssci.3.

[18] A. Ibrahim, A.A. Suleiman, U.A. Abdullahi, S.A. Suleiman, Monitoring Groundwater Quality Using Probability Distribution in Gwale, Kano State, Nigeria, J. Stat. Model. Anal. 3 (2021), 95-108. https://doi.org/10.22452/josma.vol3no2.6.

[19] A.I. Ishaq, A.A. Abiodun, A.A. Suleiman, A. Usman, A.S. Mohammed, M. Tasiu, Modelling Nigerian Inflation Rates from January 2003 to June 2023 Using Newly Developed Inverse Power Chi-Square Distribution, in: 2023 4th International Conference on Data Analytics for Business and Industry (ICDABI), IEEE, 2023, pp. 644-651. https://doi.org/10.1109/icdabi60145.2023.10629442.

[20] A.I. Ishaq, A.U. Usman, H.N. Alqifari, A. Almohaimeed, H. Daud, S.I. Abba, A.A. Suleiman, A New Log-Lomax Distribution, Properties, Stock Price, and Heart Attack Predictions Using Machine Learning Techniques, AIMS Math. 10 (2025), 12761-12807. https://doi.org/10.3934/math.2025575.

[21] A. Suleiman, A. Usman, H. Daud, F.A. Idris, R. Sokkalingam, A.I. Ishaq, A Voting Regressor Ensemble Model for Crude Oil Price Prediction, J. Stat. Sci. Comput. Intell. 1 (2025), 61-72. https://doi.org/10.64497/jssci.4.

[22] A. Usman, A.I. Ishaq, A.A. Suleiman, M. Othman, H. Daud, Y. Aliyu, Univariate and Bivariate Log-Topp-Leone Distribution Using Censored and Uncensored Datasets, Comput. Sci. Math. Forum 7 (2023), 32. https://doi.org/10.3390/iocma2023-14421.

[23] A. A. Suleiman, H. Daud, M. Othman, A. Husin, A.I. Ishaq et al. Forecasting the Southeast Asian Currencies against the British Pound Sterling Using Probability Distributions, Data Sci. Insights 1 (2023), 31-51.

[24] F. Jamal, S. Kanwal, S. Shafiq, M. Hashim, M. Kayid, M. Muhammad, S. Dutta, A.W. Shawki, The New Extended Exponentiated Burr Xii Distribution: Properties and Applications, J. Radiat. Res. Appl. Sci. 18 (2025), 101200. https://doi.org/10.1016/j.jrras.2024.101200.

[25] A.I. Ishaq, A. Usman, A.A. Suleiman, M. Othman, H. Daud, et al. Perspective Chapter: A New Bivariate Inverted Nakagami Distribution – Properties and Applications, in: New Trends and Challenges in Open Data , IntechOpen, 2023. https://doi.org/10.5772/intechopen.1001446.

[26] U. Panitanarak, A.I. Ishaq, N.S.S. Singh, A. Usman, A.U. Usman, et al. Machine Learning Models in Predicting Failure Times Data Using a Novel Version of the Maxwell Model, Eur. J. Stat. 5 (2025), 1. https://doi.org/10.28924/ada/stat.5.1.

[27] R.A.R. Bantan, F. Jamal, C. Chesneau, M. Elgarhy, Theory and Applications of the Unit Gamma/gompertz Distribution, Mathematics 9 (2021), 1850. https://doi.org/10.3390/math9161850.

[28] I. Elbatal, F. Jamal, C. Chesneau, M. Elgarhy, S. Alrajhi, The Modified Beta Gompertz Distribution: Theory and Applications, Mathematics 7 (2018), 3. https://doi.org/10.3390/math7010003.

[29] A.I. Ishaq, A.A. Suleiman, H. Daud, N.S.S. Singh, M. Othman, R. Sokkalingam, P. Wiratchotisatian, A.G. Usman, S.I. Abba, Log-kumaraswamy Distribution: Its Features and Applications, Front. Appl. Math. Stat. 9 (2023), 1258961. https://doi.org/10.3389/fams.2023.1258961.

[30] H. Semary, A.A. Suleiman, A.I. Ishaq, J.Y. Falgore, U.K. Abdullahi, H. Daud, M.A. Abd Elgawad, M. Elgarhy, A New Modified Sine-Weibull Distribution for Modeling Medical Data with Dynamic Structures, J. Radiat. Res. Appl. Sci. 18 (2025), 101427. https://doi.org/10.1016/j.jrras.2025.101427.

[31] S.F. Salleh, A.A. Suleiman, H. Daud, M. Othman, R. Sokkalingam, K. Wagner, Tropically Adapted Passive Building: a Descriptive-Analytical Approach Using Multiple Linear Regression and Probability Models to Predict Indoor Temperature, Sustainability 15 (2023), 13647. https://doi.org/10.3390/su151813647.

[32] C.K. Onyekwere, O.C. Aguwa, O.J. Obulezi, An Updated Lindley Distribution: Properties, Estimation, Acceptance Sampling, Actuarial Risk Assessment and Applications, Innov. Stat. Probab. 1 (2025), 1-27. https://doi.org/10.64389/isp.2025.01103.

[33] A.M. Gemeay, T. Moakofi, O.S. Balogun, E. Ozkan, M.M. Hossain, Analyzing Real Data by a New Heavy-Tailed Statistical Model, Mod. J. Stat. 1 (2025), 1-24. https://doi.org/10.64389/mjs.2025.01108.

[34] A.A. Suleiman, A. Suleiman, U.A. Abdullahi, S.A. Suleiman, Estimation of the Case Fatality Rate of COVID-19 Epidemiological Data in Nigeria Using Statistical Regression Analysis, Biosaf. Health 3 (2021), 4-7. https://doi.org/10.1016/j.bsheal.2020.09.003.

[35] A.A. Suleiman, H. Daud, A.G. Usman, S.I. Abba, M. Othman, M. Elgarhy, A New Two-Parameter Half-Logistic Distribution with Numerical Analysis and Applications, J. Stat. Sci. Comput. Intell. 1 (2025), 1-28. https://doi.org/10.64497/jssci.2.

[36] A.A. Suleiman, H. Daud, A.I. Ishaq, A.U. Farouk, A.S. Mohammed, M. Kayid, V.B. Nagarjuna, S. Mohammad, M. Elgarhy, A New Statistical Model for Advanced Modeling of Cancer Disease Data, Kuwait J. Sci. 52 (2025), 100429. https://doi.org/10.1016/j.kjs.2025.100429.

[37] A.I. Ishaq, A.A. Suleiman, A. Usman, H. Daud, R. Sokkalingam, Transformed Log-Burr III Distribution: Structural Features and Application to Milk Production, in: The 4th International Electronic Conference on Applied Sciences, MDPI, Basel Switzerland, 2023, pp. 322. https://doi.org/10.3390/asec2023-15289.

[38] S.O. Bashiru, M. Kayid, R. Sayed, O.S. Balogun, A. Hammad, M.A. El-Raouf, Transmuted Inverse Unit Teissier Distribution: Properties, Estimations and Applications to Medical and Radiation Sciences, J. Radiat. Res. Appl. Sci. 18 (2025), 101208. https://doi.org/10.1016/j.jrras.2024.101208.

[39] A. Usman, A.I. Ishaq, M. Tasi'U, A.A. Suleiman, U.A. Abdullahi, Inverse Power Log-Toppleone distribution and its competitors for estimating the exchange rate datasets, in: 2023 4th International Conference on Data Analytics for Business and Industry (ICDABI), IEEE, 2023, pp. 639-643. https://doi.org/10.1109/icdabi60145.2023.10629436.

[40] R.B. Yunus, N. Zainuddin, K. Kamfa, B.D. Garba, M.A. Lawan, S.I. Mohammed, An Efficient Dai-Yuan Cg Method Based on Structured Secant Conditions for Nls Problems and Its Application, J. Stat. Sci. Comput. Intell. 1 (2025), 73-84. https://doi.org/10.64497/jssci.5.

[41] B. Gompertz, On the Nature of the Function Expressive of the Law of Human Mortality, and on a New Mode of Determining the Value of Life Contingencies. In a Letter to Francis Baily, Esq. FRS &c. By Benjamin Gompertz, Esq. F. R. S., Phil. Trans. R. Soc.115 (1825), 513–583. http://doi.org/10.1098/rstl.1825.0026.

[42] N.L. Johnson, S. Kotz, N. Balakrishnan, Continuous Univariate Distributions, John Wiley & Sons, (1995).

[43] K. Ohishi, H. Okamura, T. Dohi, Gompertz Software Reliability Model: Estimation Algorithm and Empirical Validation, J. Syst. Softw. 82 (2009), 535-543. https://doi.org/10.1016/j.jss.2008.11.840.

[44] A.C. Economos, Rate of Aging, Rate of Dying and the Mechanism of Mortality, Arch. Gerontol. Geriatr. 1 (1982), 3-27. https://doi.org/10.1016/0167-4943(82)90003-6.

[45] A.C. Bemmaor, N. Glady, Modeling Purchasing Behavior with Sudden "death": A Flexible Customer Lifetime Model, Manag. Sci. 58 (2012), 1012-1021. https://doi.org/10.1287/mnsc.1110.1461.

[46] S. Dey, T. Kayal, Y.M. Tripathi, Evaluation and Comparison of Estimators in the Gompertz Distribution, Ann. Data Sci. 5 (2017), 235-258. https://doi.org/10.1007/s40745-017-0126-z.

[47] S. Dey, F.A. Moala, D. Kumar, Statistical Properties and Different Methods of Estimation of Gompertz Distribution with Application, J. Stat. Manag. Syst. 21 (2018), 839-876. https://doi.org/10.1080/09720510.2018.1450197.

[48] T. Missov, A. Lenart, Linking Period and Cohort Life-Expectancy Linear Increases in Gompertz Proportional Hazards Models, Demogr. Res. 24 (2011), 455-468. https://doi.org/10.4054/demres.2011.24.19.

[49] F.A. MOALA, S. DEY, Objective and Subjective Prior Distributions for the Gompertz Distribution, An. Acad. Bras. Ciências 90 (2018), 2643-2661. https://doi.org/10.1590/0001-3765201820171040.
[50] J.H. Pollard, E. J. Valkovics, The Gompertz Distribution and Its Applications, Genus, 48 (1992), 15-28.
[51] C. Lai, M. Xie, D. Murthy, Ch. 3. Bathtub-shaped failure rate life distributions, in: Handbook of Statistics, Elsevier, 2001, pp. 69-104. https://doi.org/10.1016/s0169-7161(01)20005-4.
[52] A. El-Gohary, A. Alshamrani, A.N. Al-Otaibi, The Generalized Gompertz Distribution, Appl. Math. Model. 37 (2013), 13-24. https://doi.org/10.1016/j.apm.2011.05.017.
[53] A. Al-Khedhairi, A. El-Gohary, A New Class of Bivariate Gompertz Distributions and Its Mixture, Int. J. Math. Anal. 2 (2008), 235-253.
[54] L.J. Bain, Analysis for the Linear Failure-Rate Life-Testing Distribution, Technometrics 16 (1974), 551-559. https://doi.org/10.2307/1267607.
[55] A.M. Sarhan, D. Kundu, Generalized Linear Failure Rate Distribution, Commun. Stat. - Theory Methods 38 (2009), 642-660. https://doi.org/10.1080/03610920802272414.
[56] M. Muhammad, B. Abba, J. Xiao, N. Alsadat, F. Jamal, M. Elgarhy, A New Three-Parameter Flexible Unit Distribution and Its Quantile Regression Model, IEEE Access 12 (2024), 156235-156251. https://doi.org/10.1109/access.2024.3485219.
[57] A.A. Jafari, S. Tahmasebi, Gompertz-power Series Distributions, Commun. Stat. - Theory Methods 45 (2015), 3761-3781. https://doi.org/10.1080/03610926.2014.911904.
[58] A.A. Jafari, S. Tahmasebi, M. Alizadeh, The Beta-Gompertz Distribution, arXiv:1407.0743 (2014). http://arxiv.org/abs/1407.0743v1.
[59] A. El-Gohary, A. Alshamrani, A.N. Al-Otaibi, The Generalized Gompertz Distribution, Appl. Math. Model. 37 (2013), 13-24.
[60] S.R. Haile, J. Jeong, X. Chen, Y. Cheng, A 3-Parameter Gompertz Distribution for Survival Data with Competing Risks, with an Application to Breast Cancer Data, J. Appl. Stat. 43 (2016), 2239-2253. https://doi.org/10.1080/02664763.2015.1134450.
[61] J. Mazucheli, A.F. Menezes, S. Dey, Unit-Gompertz Distribution with Applications, Statistica 79 (2019), 25-43. https://doi.org/10.6092/issn.1973-2201/8497.
[62] M.E. Ghitany, S.M. Aboukhamseen, A.A. Baqer, R.C. Gupta, Gompertz-lindley Distribution and Associated Inference, Commun. Stat. - Simul. Comput. 51 (2022), 2599-2618. https://doi.org/10.1080/03610918.2019.1699113.
[63] M.A.A. Boshi, S.H. Abid, N.H. Al-Noor, Generalized Gamma – Generalized Gompertz Distribution, J. Phys.: Conf. Ser. 1591 (2020), 012043. https://doi.org/10.1088/1742-6596/1591/1/012043.
[64] A.A. Suleiman, H. Daud, M. Othman, A.I. Ishaq, R. Indawati, M.L. Abdullah, A. Husin, The Odd Beta Prime-G Family of Probability Distributions: Properties and Applications to Engineering and Environmental Data, Comput. Sci. Math. Forum 7 (2023), 20. https://doi.org/10.3390/iocma2023-14429.
[65] A.A. Suleiman, H. Daud, A.I. Ishaq, M. Kayid, R. Sokkalingam, Y. Hamed, M. Othman, V.B. Nagarjuna, M. Elgarhy, A New Weibull Distribution for Modeling Complex Biomedical Data, J. Radiat. Res. Appl. Sci. 17 (2024), 101190. https://doi.org/10.1016/j.jrras.2024.101190.

[66] H. Daud, A.A. Suleiman, A.I. Ishaq, N. Alsadat, M. Elgarhy, A. Usman, P. Wiratchotisatian, U.A. Ubale, Y. Liping, A New Extension of the Gumbel Distribution with Biomedical Data Analysis, J. Radiat. Res. Appl. Sci. 17 (2024), 101055. https://doi.org/10.1016/j.jrras.2024.101055.

[67] A.A. Suleiman, H. Daud, A.I. Ishaq, M. Othman, H.M. Alshanbari, S.N. Alaziz, A Novel Extended Kumaraswamy Distribution and Its Application to COVID-19 Data, Eng. Rep. 6 (2024), e12967. https://doi.org/10.1002/eng2.12967.

[68] A.A. Suleiman, H. Daud, A.I. Ishaq, M. Othman, R. Sokkalingam, A. Usman, A.A. Osi, The Odd Beta Prime Inverted Kumaraswamy Distribution with Application to COVID-19 Mortality Rate in Italy, in: The 4th International Electronic Conference on Applied Sciences, MDPI, Basel Switzerland, 2023, pp. 218. https://doi.org/10.3390/asec2023-16310.

[69] A.A. Suleiman, H. Daud, N.S.S. Singh, A.I. Ishaq, M. Othman, A New Odd Beta Prime-Burr X Distribution with Applications to Petroleum Rock Sample Data and Covid-19 Mortality Rate, Data 8 (2023), 143. https://doi.org/10.3390/data8090143.

[70] A.A. Suleiman, H. Daud, O. Mahmod, N. Singh, A Novel Extension of the Fréchet Distribution: Statistical Properties and Application to Groundwater Pollutant Concentrations, Data Sci. Insights, 1 (2023), 8-24.

[71] A.A. Suleiman, H. Daud, N.S.S. Singh, M. Othman, A.I. Ishaq, R. Sokkalingam, A Novel Odd Beta Prime-Logistic Distribution: Desirable Mathematical Properties and Applications to Engineering and Environmental Data, Sustainability 15 (2023), 10239. https://doi.org/10.3390/su151310239.

[72] A.S. Alghamdi, M.M. Abd El-Raouf, Exploring the Dynamics of Covid-19 with a Novel Family of Models, Mathematics 11 (2023), 1641. https://doi.org/10.3390/math11071641.

[73] A.M.T. Abd El-Bar, I.E. Ragab, On Weighted Exponential-Gompertz Distribution: Properties and Application, J. Taibah Univ. Sci. 13 (2019), 616-627. https://doi.org/10.1080/16583655.2019.1600277.

[74] M. Shama, S. Dey, E. Altun, A.Z. Afify, The Gamma–gompertz Distribution: Theory and Applications, Math. Comput. Simul. 193 (2022), 689-712. https://doi.org/10.1016/j.matcom.2021.10.024.

[75] A.I. Ishaq, U. Panitanarak, A.A. Abiodun, A.A. Suleiman, H. Daud, The Generalized Odd Maxwell-Kumaraswamy Distribution: Its Properties and Applications, Contemp. Math. (2024), 711-742. https://doi.org/10.37256/cm.5120242888.